Charles University in Prague
Faculty of Mathematics and Physics

DIPLOMA THESIS

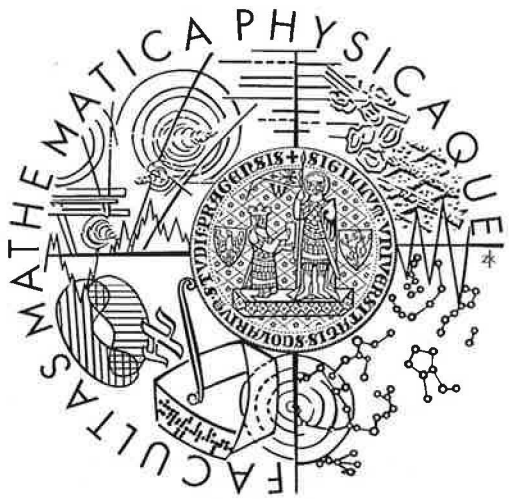

Miroslav Šulc

Numerical solution of scattering integral equations

Institute of Theoretical Physics
Supervisor: Prof. RNDr. Jiří Horáček, DrSc.
Study program: Theoretical physics

Na tomto místě bych rád poděkoval zejména vedoucímu práce prof. J. Horáčkovi za vytvoření přímo luxusního zázemí jak po teoretické tak po materiální stránce pro realizaci této práce a též P. Kolorenčovi za cenné konzultace.

I hereby declare that this diploma thesis has been created by myself and by use of the referenced literature only.

Prague, April 13, 2007 Miroslav Šulc

Contents

Název práce: Numerické řešení integrálních rovnic teorie rozptylu
Autor: Miroslav Šulc
Katedra (ústav): Ústav teoretické fyziky
Vedoucí diplomové práce: Prof. RNDr. Jiří Horáček, DrSc.
E-mail vedoucího: horacek@mbox.troja.mff.cuni.cz

Abstrakt: Tato práce se zabývá studiem několika vybraných numerických metod řešení integrální formy Lippmann-Schwingerovy rovnice pro potenciálový rozptyl v rámci nerelativistické kvantové teorie. Na vybraných modelech je studována efektivita spolu s konvergenčními vlastnostmi jednotlivých metod. Testované algoritmy jsou následně použity mimo jiné k výpočtu parametrů charakterizujících rozptylový proces v daných případech.
Klíčová slova: Lippmannova–Schwingerova rovnice, R-matice, rozptylový problém

Title: Numerical solution of scattering integral equations
Author: Miroslav Šulc
Department: Institute of Theoretical Physics
Supervisor: Prof. RNDr. Jiří Horáček, DrSc.
Supervisor's e-mail address: horacek@mbox.troja.mff.cuni.cz

Abstract: In the present work we are concerned mainly with the study of several methods for numerical solution of the Lippmann-Schwinger equation for potential scattering in the framework of the non relativistic quantum theory. For several model cases, we study the effectiveness and consequently the convergence properties of the presented methods. The tested algorithms are then applied to the computation of the quantities characterizing the scattering process in given cases.

Keywords: Lippmann–Schwinger equation, R-matrix, scattering problem

Chapter 1

Introduction

It is notoriously difficult to obtain reliable results for quantum mechanical scattering problems. Since they involve complicated interference phenomena of waves, any simple uncontrolled approximation is not worth more than the weather forecast. However, for two body problems with central forces the computer can be used to compute the phase shifts.

W. Thirring

1.1 Formulation of the problem

In this work, we are concerned with the non relativistic potential scattering, especially with numerical description of the corresponding equations. In the framework of this subject, the "master" equation is the well-known Lippmann-Schwinger equation, originally published in [14]. In symbolic manner, one can write it in the integral form

$$T = V + VG_0(E)T, \tag{1.1}$$

where T stands for the transition operator, which is often defined by acting on the source term (incident plane wave with energy E) as $T|\varphi\rangle = H_I|\phi\rangle$, where H_I denotes the interaction Hamiltonian and $|\phi\rangle$ has the meaning of the complete solution of the scattering problem under consideration. The most naive approach to cope with equation (1.1) would be an iterative method yielding $T = V + VG_0(E)V + \ldots$. Unfortunately, it often turns out, that this series diverges making this approach useless. In this case, more reliable methods are required to handle the scattering problem correctly. The aim of the following chapters is to describe few of them and study consequently their properties...

Chapter 2

Overview of the numerical approaches

The aim of all the methods given below in this section is to calculate the T-matrix (also known as the transition operator) in momentum space as function of initial and final momentum vectors for different type of potentials. Common approach to this issue lies in the decomposition of the Lippmann-Schwinger equation (1.1) into partial waves. This seems to be a reasonable strategy for low energies and short range potentials, because only a few partial waves are needed to fully describe the properties of the scattering process in this case. However, for higher energies, the separate partial-wave components oscillate typically strongly in the scattering angle, whereas the total scattering amplitude is a relatively smooth function. This suggests, that an effective numerical determination of the T-matrix could be a handy tool.

2.1 Nyström method

Roughly speaking, the core of this method is to rewrite the Lippman-Schwinger equation (1.1) in the momentum representation and convert it to a set of linear algebraic equations. However, a special care has to be taken about the singularity in the kernel of the corresponding integral equation arising from the presence of the free propagator. The matrix elements of the two body T-matrix obey the following integral equation, which can be seen to be a Fredholm integral equation of the second kind with its kernel determined by the product of the model potential and the free propagator.

$$T(\vec{q}', \vec{q}, z) = V(\vec{q}', \vec{q}) + \int \mathrm{d}^3\vec{q}'' V(\vec{q}', \vec{q}'') \frac{1}{z - \frac{q''^2}{m}} T(\vec{q}'', \vec{q}, z), \tag{2.1}$$

where m stands for the reduced mass of the two body problem. In this notation the T-matrix is thought to be a complex function of the (complex) variable z. In

the case of two spin less particles and local spherically symmetric potentials the matrix elements of the potential $V(\vec{q}', \vec{q})$ as well as the matrix elements of the sought T-matrix $T(\vec{q}', \vec{q}, z)$ will be scalar functions, i.e.

$$V(\vec{q}', \vec{q}) = V(q', q, \widehat{q}' \cdot \widehat{q})$$

$$T(\vec{q}', \vec{q}, z) = T(q', q, \widehat{q}' \cdot \widehat{q}, z),$$

where for example the notation $\widehat{q}$ denotes the unit vector in the direction of $\vec{q}$. Incorporating this assumption into the equation (2.1) then yields

$$T(q', q, x') = V(q', q, x') + \int_0^\infty \mathrm{d}q'' q''^2 \int_{-1}^1 \mathrm{d}x'' \int_0^{2\pi} \mathrm{d}\phi'' \frac{mV(q', q'', y)T(q'', q, x'')}{q^2 - q''^2 + i\epsilon}, \tag{2.2}$$

where $x' = \widehat{q}' \cdot \widehat{q}$, $x'' = \widehat{q}'' \cdot \widehat{q}$ and $y = \widehat{q}'' \cdot \widehat{q}'$. Nevertheless the quantity y can be easily expressed via x' and x'' by means of some simple geometry as

$$y = x'x'' + \sqrt{1 - x'^2}\sqrt{1 - x''^2}\cos\phi''.$$

In terms of

$$v(q', q, x', x) \equiv \int_0^{2\pi} \mathrm{d}\varphi V(q', q, x'x + \sqrt{1 - x'^2}\sqrt{1 - x^2}\cos\varphi), \tag{2.3}$$

the equation (2.1) can be then rewritten in its final form which is then handled numerically.

$$T(q', q, x') = \frac{1}{2\pi} v(q', q, x', 1) + m \int_0^\infty \mathrm{d}q'' q''^2 \int_{-1}^1 \mathrm{d}x'' \frac{v(q', q'', x', x'')}{q - q''^2 + i\epsilon} T(q'', q, x''). \tag{2.4}$$

Indeed, substituting 1 for x in the equation (2.3) yields

$$v(q', q, x', 1) = \int_0^{2\pi} \mathrm{d}\varphi V(q', q, x') = 2\pi V(q', q, \widehat{q}' \cdot \widehat{q})$$

In equation (2.4), we have already used the retarded form of the free propagator, i.e. $z = (q_0^2/m) + i\epsilon$, where q_0 corresponds to the incoming momentum. Natural question arising at this point is how to treat properly the singular term in (2.4). The following technique has been used in this work.
First of all, the $1/(x + i\epsilon)$ term is decomposed by the means of the following formula

$$\frac{1}{x + i\epsilon} = \mathrm{P}\frac{1}{x} - i\frac{\pi}{2}\delta(x), \tag{2.5}$$

yielding

$$T(q',q,x') = \frac{1}{2\pi}v(q',q,x',1) + m\int_0^\infty \mathrm{d}q'' \int_{-1}^{1}\mathrm{d}x'' q''^2 \frac{v(q',q'',x',x'')}{q_0^2 - q''^2 + i\epsilon} T(q'',q,x'')$$
$$= \frac{1}{2\pi}v(q',q,x',1) + m\mathrm{P}\!\int_0^\infty \mathrm{d}q'' \int_{-1}^{1}\mathrm{d}x'' q''^2 \frac{v(q',q'',x',x'')}{q_0^2 - q''^2} T(q'',q,x'')$$
$$- i\frac{\pi}{2}mq_0\int_{-1}^{1}\mathrm{d}x'' v(q'',q_0,x',x'')T(q_0,q,x''). \quad (2.6)$$

As usual, the symbol P$\int$ denotes the Cauchy principal value integral.
Consequently a trick due to Sloan [2, p. 114] is used to handle the first integral in the equation (2.6) maintaining the consistency with the principal value limit. The integration range of the radial part of momentum is transformed via following bilinear mapping

$$y = \frac{q - q_0}{q + q_0}, \quad (2.7)$$

where the images of the points $q = 0, q_0, \infty$ are $y = -1, 0, 1$ as part of the mapping of $0 \leq q \leq \infty$ into $-1 \leq y \leq 1$. Finally, the whole two dimensional integral equation can be discretized using Gauss Legendre quadrature rule. Because of the well know fact, that the quadrature nodes of the Gauss-Legendre quadrature rule are localized symmetrically about the center of the interval of integration, an even number of mesh points were used as concerns the discretization of the radial part of the momentum. This choice has two consequences. It avoids the point q_0 to be a mesh point and thanks to the mentioned symmetry of the quadrature rule it handles correctly the p.v.-limit. Further discussion is left into the next chapter.

2.2 Nyström-Chebyshev method

This method constitutes an improvement to the previous method based on direct quadrature. The refinement rests on the way how the singularity in the integral kernel (in equation (2.4)) is handled. In principle, the core of the presented method is based on the two following identities according to [1]

$$\mathrm{P}\!\int_{-1}^{1}\mathrm{d}x \frac{T_n(x)}{x-y}\frac{1}{\sqrt{1-x^2}} = \begin{cases} \pi U_{n-1}(y) & n \geq 1 \\ 0 & n = 0 \end{cases}$$

$$\mathrm{P}\!\int_{-1}^{1}\mathrm{d}x \frac{U_n(x)}{x-y}\sqrt{1-x^2} = -\pi T_{n+1}(y), \text{ where } n \in \mathbf{N}_0 \text{ and } |y| < 1, \quad (2.8)$$

where T_n resp. U_n are Chebyshev polynomials of the first resp. of the second kind. To be able to benefit from these identities, we would need to expand somehow the kernel of the LS equation under consideration as well as the sought solution into

series of Chebyshev polynomials and consequently find relations determining the coefficients in these series, solving of which would give us an approximation to the final solution. This approach is described below.

Because of the similarity with the previous method we give here a brief description of this algorithm in the same notation as in the previous case. Assuming once again, that the sought T-matrix is a scalar function of its arguments, we can write down the LS equation in the following form

$$\begin{aligned} T(q',q,x') &= \frac{1}{2\pi}v(q',q,x',1) + m\int_0^\infty \mathrm{d}q'' \int_{-1}^{1} \mathrm{d}q'' q''^2 \frac{v(q',q'',x',x'')}{q_0^2 - q''^2 + i\epsilon} T(q'',q,x'') \\ &= \frac{1}{2\pi}v(q',q,x',1) + m\mathrm{P}\int_0^\infty \mathrm{d}q'' \int_{-1}^{1} \mathrm{d}x'' q''^2 \frac{v(q',q'',x',x'')}{q_0^2 - q''^2} T(q'',q,x'') \\ &\quad - i\frac{\pi}{2} m q_0 \int_{-1}^{1} \mathrm{d}x'' v(q'',q_0,x',x'') T(q_0,q,x''), \end{aligned} \tag{2.9}$$

where q_0 denotes the radial part of the incoming momentum as usual.

The only term which poses again a numerical difficulty is the second one (the double integral over q'' and x''). In order to cope with this difficulty, we utilize the following nonlinear transformation

$$q'' = C\left[\frac{1+y''}{1-y''}\right]^{1/2}, \tag{2.10}$$

or equivalently

$$y'' = \frac{q''-C^2}{q''+C^2}, \tag{2.11}$$

where C is assumed to be a positive real constant.

By defining $\kappa = mC^3/(q_0^2+C^2)$ together with

$$F(y',y'',x',x'') \equiv v(y',y'',x',x'')\frac{(1+y'')^{1/2}}{(1-y'')^{3/2}} \tag{2.12}$$

and implementing substitution (2.10), the mentioned problematic term in (2.9) can be restated as

$$\kappa\mathrm{P}\int_{-1}^{1}\mathrm{d}y'' \int_{-1}^{1}\mathrm{d}x'' F(y',y'',x',x'')\frac{T(y'',y,x'')}{y_0 - y''}. \tag{2.13}$$

Next, we introduce following notation and consequently expand this expression understood as a function of y'' in terms of Chebyshev polynomials of the first kind. Explicitly written, we obtain

$$\begin{aligned} f(y',y;y'',x',x'') &\equiv \sqrt{1-y''^2}F(y',y'',x',x'')T(y'',y,x'') \approx \\ &\approx \sum_1^N a_n(y',y;y_0,x',x'')T_n(y''). \end{aligned} \tag{2.14}$$

It is worth to note, that the absolute term ($n = 0$) is not considered, because it won't contribute in the final stage to the integral under investigation. The other coefficients a_n for $n > 1$ are determined in usual manner as

$$a_n(y', y; y_0, x', x'') = \frac{2}{\pi} \int_{-1}^{1} \mathrm{d}y'' F(y', y'', x', x'') T(y'', y, x'') T_n(y''). \tag{2.15}$$

Incorporating this definition into the expression (2.13) yields

$$\begin{aligned} \kappa \mathrm{P} \int_{-1}^{1} \mathrm{d}y'' \int_{-1}^{1} \mathrm{d}x'' \sum_{1}^{N} a_n(y', y; y_0, x', x'') \frac{T_n(y'')}{\sqrt{1 - y''^2}} \frac{1}{y_0 - y''} = \\ = -\kappa \int_{-1}^{1} \mathrm{d}x'' \sum_{1}^{N} a_n(y', y; y_0, x', x'') \pi U_{n-1}(y_0), \end{aligned} \tag{2.16}$$

where the second of the two identities (2.8) has been used. In order to discretize the defining relation (2.15) for the coefficients a_n, we make use of the M–point Gauss–Chebyshev quadrature rule, i.e. rule with weight function $w(x) = (1 - x^2)^{-1/2}$. The appropriate weights and nodes are given as

$$w_i \equiv w = \frac{\pi}{M} \qquad\qquad y_i = \cos\left(\frac{2i - 1}{2} w\right). \tag{2.17}$$

Inserting in equation (2.15) yields

$$\begin{aligned} a_n(y', y; y_0, x', x'') &= \frac{2}{\pi} \sum_{1}^{M} w_i \sqrt{1 - y_i^2} F(y', y_i, x', x'') T(y_i, y, x'') T_n(y_i) = \\ &= \frac{2}{\pi} \sum_{1}^{M} v(y', y_i, x', x'') \frac{1 + y_i}{1 - y_i} T(y_i, y, y'') T_n(y_i). \end{aligned} \tag{2.18}$$

Thus the final discretized form of the original LS equation can be written as

$$\begin{aligned} T(y_k, y_k, x_l) = \frac{1}{2\pi} v(y_k, y_k, x_l, 1) - i\frac{\pi}{2} m q_0 \sum_{j=1}^{N_x} w_j^x v(y_k, y_0, x_l, x_j) T(y_0, y_k, x_j) \\ - \frac{2\kappa\pi}{M} \sum_{n=1}^{N} \sum_{i=1}^{M} \sum_{j=1}^{N_x} w_j^x v(y_k, y_i, x_l, x_j) \frac{1 + y_i}{1 - y_i} T(y_i, y_k, x_j) T_n(y_i) U_{n-1}(y_0), \end{aligned} \tag{2.19}$$

where the integration over x'' has been already replaced by means of the N_x–point Gauss–Legendre quadrature rule. Equation (2.19) represents a system of linear equations for the unknown values of the on-shell T-matrix element at the integration nodes. This system of equations is then solved in standard manner. In our implementation we have chosen the pivoted LU decomposition.

2.3 R-matrix and Lanczos method

Typical model potential U consists of a local V and a nonlocal part W. This rather arbitrary decomposition seems to be of limited usefulness. Nevertheless it turns out, that the converse is true. The main idea of this method is to handle the two mentioned terms separately.
Inserting the mentioned potential decomposition into the original LS equation (2.4) yields

$$|\phi\rangle = |u\rangle + G_0(E)(V+W)\,|\phi\rangle\,, \tag{2.20}$$

where the "source" term $|u\rangle$ describes the incident plane wave and $G_0(E)$ stands for the free propagator corresponding to energy E. Some simple algebraic manipulations furnish an another insight onto this equation. Explicitly written

$$\begin{aligned} |\phi\rangle &= (1 - G_0(E)V)^{-1}\,|u\rangle + (1 - G_0(E)V)^{-1}G_0(E)W\,|\phi\rangle \\ &\equiv |\overline{u}\rangle + G(E)W\,|\phi\rangle\,, \end{aligned} \tag{2.21}$$

where $|\overline{u}\rangle$ has the meaning of the distorted wave obeying following equation

$$|\overline{u}\rangle \stackrel{\text{def}}{=} |u\rangle + G_0(E)V\,|\overline{u}\rangle \tag{2.22}$$

and $G(E)$ is the Green's function of the distorted wave, namely

$$G(E) \stackrel{\text{def}}{=} (1 - G_0(E)V)^{-1}G_0(E) \tag{2.23}$$

Equation (2.21) takes the same form as the equation (2.22) only with the replacement $|u\rangle \to |\overline{u}\rangle$ and $G_0(E) \to G(E)$. In the description of the scattering process, we are mainly concerned in the quantity $\langle u|\,V + W\,|\phi\rangle$. But this can be shown by means of simple algebra to be equal to $\langle u|\,V\,|\overline{u}\rangle + \langle\overline{u}|\,W\,|\phi\rangle$, so it is sufficient to solve the partial problems separately, according to the following "algorithm".

1. solve the LS equation with source term $|u\rangle$ considering only the local potential using the R-matrix method obtaining the solution $|\overline{u}\rangle$ according to the following recipe
   (a) write the sought solution $|\overline{u}\rangle$ as a sum of two parts $|\overline{u}\rangle = |u\rangle + |\xi\rangle$
   (b) $|\overline{u}\rangle$ is also an eigenvector corresponding to the energy E of the Hamiltonian $H_V = K_T + V$, where K_T is the operator of kinetic energy of free particle with reduced mass μ, so the following relations hold

$$\begin{aligned} (K_T + V)\,\{|u\rangle + |\xi\rangle\} &= E\,\{|u\rangle + |\xi\rangle\} \\ V\,|u\rangle + H_V\,|\xi\rangle &= E\,|\xi\rangle \\ |\xi\rangle &= (E - H_V)^{-1}V\,|u\rangle = G(E)V\,|u\rangle\,, \end{aligned}$$

where the notation $G(E)$ has been used for the quantity $(E - H_V)^{-1}$ because of the fact, that it is exactly the same as $(1-G_0(E)V)^{-1}G_0(E)$. This observation can be checked immediately by means of the following general operator identity $(\hat{A} - \hat{B})^{-1} = \hat{A}^{-1} + \hat{A}^{-1}\hat{B}(\hat{A} - \hat{B})^{-1}$.

2. consequently obtain the solution $|\overline{u}\rangle$ as sum of the source term $|u\rangle$ and the vector obtained by acting of the Green's function $G(E)$ on the ket $V|u\rangle$. The Green's function is constructed via the R-matrix method as described below. The machinery of this method ensures, that the desired boundary condition at the end of the integration interval is correctly incorporated into the Green's function under construction.

3. solve the LS equation with source term $|\overline{u}\rangle$ with nonlocal potential only by the means of Schwinger-Lanczos iterative algorithm obtaining the final solution $|\phi\rangle$ and also the T-matrix element as a byproduct of the iterative procedure.

2.3.1 One dimensional R-matrix method

In the case of partial wave decomposition one has to cope typically with following second order differential equation

$$-\frac{1}{2\mu}\frac{\mathrm{d}^2\Psi(r)}{\mathrm{d}r^2} + (V_{eff}(r) - E)\Psi(r) = \chi(r) \tag{2.24}$$

with boundary conditions

$$\Psi(0) = 0, \qquad \left(A - \frac{\mathrm{d}}{\mathrm{d}r}\right)\Psi(r)\Big|_{r_f} = 0, \tag{2.25}$$

where r_f lies in a region, where neglecting the potential is plausible and A is an arbitrary constant.

In the first step of this method a suitable basis is to be found. The elements of this basis are required to be eigenfunctions of operator $\tilde{K} + V_{eff}(r)$, i.e.

$$\tilde{K}\Psi_n(r) + (V_{eff}(r) - E_n)\Psi_n(r) = 0. \tag{2.26}$$

$\tilde{K}$ is the so called operator of modified kinetic energy and is usually written in the form $\tilde{K} = \frac{1}{2\mu}\frac{\mathrm{d}^2}{\mathrm{d}r^2} + L$, where L denotes the *Bloch operator*. It is defined as

$$L_{ij} = \frac{1}{2\mu}\Psi_i(r_f)\left.\frac{\mathrm{d}\Psi_j(r)}{\mathrm{d}r}\right|_{r_f}. \tag{2.27}$$

Its domain of definition is the space of square integrable functions satisfying the boundary condition (2.25) at the origin. Utilizing integration per partes and the

mentioned boundary condition gives for the matrix elements of the modified kinetic energy

$$\tilde{K}_{ij} = \frac{1}{2\mu}\int_0^{r_f} \frac{\mathrm{d}\Psi_i(r)}{\mathrm{d}r}\frac{\mathrm{d}\Psi_j(r)}{\mathrm{d}r}\mathrm{d}r. \tag{2.28}$$

So the operator $\tilde{K} + V_{eff}(r)$ is symmetric, thus has real eigenvalues E_n and its eigenvectors $\Psi_n(r)$ build basis of the function space under consideration. Incorporating the definition of Bloch operator into equation (2.24) yields

$$\tilde{K}\Psi(r) + (V(r) - E)\Psi(r) = \chi(r) + L\Psi(r). \tag{2.29}$$

By expanding the function $\Psi(r)$ into basis $\Psi_n(r)$ as $\Psi(r) = \sum_n C_n\Psi_n(r)$ and plugging into previous equation a relation for the coefficients C_n is obtained

$$C_n = \frac{1}{E_n - E}\left[\chi_n + \frac{1}{2\mu}\Psi_n(r_f)\lambda\right], \tag{2.30}$$

where

$$\chi_n = \int_0^{r_f} \Psi_n(r)\chi(r)\mathrm{d}r$$

and the parameter λ is equal to the logarithmic derivative of the complete wave function $\Psi(r)$ at $r = r_f$, i.e.

$$\lambda = \left.\frac{\mathrm{d}\Psi(r)}{\mathrm{d}r}\right|_{r_f}.$$

It can be related to the parameter A introduced in (2.25) utilizing the equation for the expansion coefficients (2.30). Particularly

$$\lambda = \frac{A}{1 - A\mathcal{R}}\sum_k \frac{\chi_k\Psi_k(r_f)}{E_k - E}, \tag{2.31}$$

where $\mathcal{R}$ stands for

$$\mathcal{R} = \frac{1}{2\mu}\sum_n \frac{\Psi_n(r_f)\Psi_n(r_f)}{E_n - E}.$$

This function of r_f has a direct physical meaning. It can be shown, that it is equal to the inverse logarithmic derivative of the complete wave function at the edge of the interval of integration, i.e. $r = r_f$. Its knowledge is sufficient in the one dimensional case to compute the T-matrix directly without the need to compute numerically the integral $\langle\chi|\, V\,|\Psi\rangle$.

At this point, the equation (2.24) is solved completely, because the explicit form of the coefficients C_n is known. However, the solution can be expressed in a slightly different way more suitable for computation according to [16]. Namely

$$\Psi(r) = \int_0^{r_f} G(E, r, r')\chi(r')\mathrm{d}r', \tag{2.32}$$

where $G(E,r,r')$ is indeed the Green's function of the original equation (2.24) being the solution of this equation for the source term $\chi(r) = \delta(r-r')$. Explicitly ([16])

$$G(E,r,r') = \sum_n \frac{\Psi_n(r)\Psi_n(r')}{E_n - E} + \frac{A}{2\mu(1-A\mathcal{R})} \sum_{n,m} \frac{\Psi_n(r)\Psi_n(r_f)\Psi_m(r_f)\Psi_m(r')}{(E_n-E)(E_m-E)}. \tag{2.33}$$

However, if the range of integration is required to be large (for example due to higher energy or long range potential), more and more basis functions are to be taken into account to describe the scattering process properly thus increasing the computational complexity. This drawback can be bypassed partially by decomposition of the whole radial interval $\langle 0, r_f\rangle$ into several subsectors.

In this case, the Bloch operator is defined on each subsector as

$$L_{ij}^{(n)} = \frac{1}{2\mu}\left(\Psi_i(r_n)\left.\frac{\mathrm{d}\Psi_j(r)}{\mathrm{d}r}\right|_{r_n} - \Psi_i(r_{n-1})\left.\frac{\mathrm{d}\Psi_j(r)}{\mathrm{d}r}\right|_{r_{n-1}}\right). \tag{2.34}$$

The strategy is then similar as in the one sector case. Analogously, the wave function is decomposed as

$$\Psi(r) = \sum_k C_k^{(n)}\Psi_k^{(n)}(r), \qquad r \in \langle r_{n-1}, r_n\rangle, \tag{2.35}$$

where the coefficients $C_k^{(n)}$ are determined by the relation

$$C_k^{(n)} = \frac{1}{E_k^{(n)} - E}\left[\chi_k^{(n)} + \frac{1}{2\mu}\Psi_k^{(n)}(r_n)\lambda^{(n)} - \frac{1}{2\mu}\Psi_k^{(n)}(r_{n-1})\mu^{(n)}\right], \tag{2.36}$$

where

$$\chi_k^{(n)} = \int_{r_{n-1}}^{r_n} \Psi_k^{(n)}(r)\chi(r)\mathrm{d}r \tag{2.37}$$

$$\lambda^{(n)} = \left.\frac{\mathrm{d}\Psi(r)}{\mathrm{d}r}\right|_{r_n}, \qquad \mu^{(n)} = \left.\frac{\mathrm{d}\Psi(r)}{\mathrm{d}r}\right|_{r_{n-1}}. \tag{2.38}$$

Because it is assumed that $\Psi(r) \in C^1(0; r_f)$, we get $\mu^{(n)} = \lambda^{(n-1)}$ for $n = 2, \cdots, N_s$, where N_s denotes the total count of subsectors. This fact together with the boundary condition at the origin gives following relations for the expansion coefficients

$$C_k^{(1)} = \frac{1}{E_k^{(1)} - E}\left[\chi_k^{(1)} + \frac{1}{2\mu}\Psi_k^{(1)}(r_1)\lambda^{(1)}\right] \tag{2.39}$$

$$C_k^{(n)} = \frac{1}{E_k^{(n)} - E}\left[\chi_k^{(n)} + \frac{1}{2\mu}\Psi_k^{(n)}(r_n)\lambda^{(n)} - \frac{1}{2\mu}\Psi_k^{(n)}(r_{n-1})\lambda^{(n-1)}\right] \tag{2.40}$$

The coefficients λ_i are then determined by the requirement of continuity of the sought wave function and the boundary condition at $r = r_f$. By denoting

$$ {}^{r}\chi^{(n)} = \sum_k \frac{\chi_k^{(n)}\Psi_k^{(n)}(r_n)}{E_k^{(n)} - E}, \qquad {}^{l}\chi^{(n)} = \sum_k \frac{\chi_k^{(n)}\Psi_k^{(n)}(r_{n-1})}{E_k^{(n)} - E} \tag{2.41} $$

$$ R^{(n)} = \frac{1}{2\mu}\sum_k \frac{\Psi_k^{(n)}(r_n)\Psi_k^{(n)}(r_n)}{E_k^{(n)} - E} \tag{2.42} $$

$$ M^{(n)} = \frac{1}{2\mu}\sum_k \frac{\Psi_k^{(n)}(r_n)\Psi_k^{(n)}(r_{n-1})}{E_k^{(n)} - E} \tag{2.43} $$

$$ L^{(n)} = \frac{1}{2\mu}\sum_k \frac{\Psi_k^{(n)}(r_{n-1})\Psi_k^{(n)}(r_{n-1})}{E_k^{(n)} - E}, \tag{2.44} $$

we obtain the following final set of linear equations

$$ \begin{aligned} M^{(2)}\lambda^{(2)} - (L^{(2)} + R^{(1)})\lambda^{(1)} &= {}^{r}\chi^{(1)} - {}^{l}\chi^{(2)}, \\ M^{(n+1)}\lambda^{(n+1)} - (L^{(n+1)} + R^{(n)})\lambda^{(n)} + M^{(n)}\lambda^{(n-1)} &= {}^{r}\chi^{(n)} - {}^{l}\chi^{(n+1)} \\ &\text{where } n = 2, \ldots, N_s - 1 \\ \frac{1 - A\mathcal{R}^{(N)}}{A}\lambda^{(N)} + M^{(N)}\lambda^{(N-1)} &= {}^{r}\chi^{(N)}. \end{aligned} \tag{2.45} $$

If we wish to use the benefit of knowledge of the inverse logarithmic derivate of the solution of the homogeneous Schrödinger equation as in the previous case, a little bit more calculations are needed, because the quantity (2.42) has this meaning only at the right edge of the first sector, i.e. at $r = r_1$. Nevertheless, according to [16], following recurrence will do the job

$$ \begin{aligned} \mathcal{R}^{(n)} &= R^{(n)} - M^{(n)}\frac{1}{\mathcal{R}^{(n-1)} + L^{(n)}}M^{(n)}, \\ \mathcal{R}^{(1)} &= R^{(1)}. \end{aligned} \tag{2.46} $$

To write explicitelly the Green's function in this case would require to solve the set of equations (2.45) analytically. Final expression would be then rather cumbersome and in the eye of the numerical computation of limited use. More efficient is to solve the tridiagonal set of equations (2.45) numerically, compute the expansion coefficients and consequently reconstruct the sought wave function.

2.3.2 Schwinger-Lanczos variational method

Schwinger-Lanczos method is an iterative approach to the problem of calculation the T-matrix elements. It relies on the complex Schwinger variational principle

as described in the original work [14]. According to this principle, the desired T-matrix element

$$T_{\beta\alpha} = \langle\phi_\beta| (1 - VG_0)^{-1} V |\phi_\alpha\rangle = \langle\phi_\beta| V(V - VG_0V)^{-1} V |\phi_\alpha\rangle$$

is given as stationary value of following functional

$$T[\psi_-, \psi_+] = \langle\phi_\beta| V |\psi_+\rangle + \langle\psi_-| V |\phi_\alpha\rangle - \langle\psi_-| V - VG_0V |\psi_+\rangle .$$

It can be shown, that this functional takes its stationary value for ψ_-, ψ_+ being the corresponding solutions of the LS equation. The main idea of this method is to choose a suitable basis, expand the sought solutions into this basis, write equations for these coefficients and consequently construct the original solutions.

If we denote the basis under consideration as $\{|g_k\rangle\}_{k=1}^N$ and the variational coefficients as $c_k^{(\pm)}$, then we can write

$$|\psi_\pm\rangle = \sum_{k=1}^{N} c_k^{(\pm)} |g_k\rangle .$$

The final T-matrix element is then approximated as

$$T_{\beta\alpha}^N = \sum_{k,l=1}^{N} \langle\phi_\beta| V |g_k\rangle \left(M^{-1}\right)_{kl} \langle g_l| V |\phi_\alpha\rangle , \tag{2.47}$$

where the elements of the matrix M are given as $M_{kl} = \langle g_k| V - VG_0V |g_l\rangle$. Although the choice of the basis seems to be quite appropriate, it is a fundamental ingredient of this method. In principle, all we need is the matrix M being regular. However, this requirement is only a necessary and not a sufficient condition on the basis to be suitable for fast convergence of the entire method.

According to [15] it turns out to be convenient to construct the basis so as to be "V-orthogonal", that is

$$\langle g_k| V |g_l\rangle = \delta_{kl}$$

and in addition the matrix VG_0V is required to be tridiagonal, i.e.

$$\begin{aligned} \langle g_{k-1}| VG_0V |g_k\rangle = \langle g_k| VG_0V |g_{k-1}\rangle &= \beta_{k-1} \\ \langle g_k| VG_0V |g_k\rangle &= \alpha_k \\ \langle g_k| VG_0V |g_l\rangle &= 0, \text{ for } |k-l| \geq 2. \end{aligned} \tag{2.48}$$

The basis, that fulfills these conditions is constructed iteratively with the first vector chosen in the form $|g_1\rangle = \langle\phi| V |\phi\rangle^{-1/2}$. Because the basis under construction is required to be V-orthogonal, only the matrix element $(M^{-1})_{11}$ is required in the

equation (2.47). Some rather tedious calculations furnish this element in the form of a continued fraction, namely

$$T^N = \langle\phi| V |g_1\rangle \left(M^{-1}\right)_{11} \langle g_1| V |\phi\rangle = \cfrac{\langle\phi| V |\phi\rangle}{1 - \alpha_1 - \cfrac{\beta_1^2}{1 - \alpha_2 - \cfrac{\beta_2^2}{1 - \alpha_3 - \cdots \cfrac{\beta_{N-1}^2}{1 - \alpha_N}}}} \tag{2.49}$$

Complete recurrent relations according to [15] are

$$|r_k\rangle = G_0 V |g_k\rangle - \beta_{k-1} |g_{k-1}\rangle , \tag{2.50}$$

$$\alpha_k = \langle g_k| V |r_k\rangle , \tag{2.51}$$

$$|s_k\rangle = |r_k\rangle - \alpha_k |g_k\rangle , \tag{2.52}$$

$$\beta_k = \langle s_k| V |s_k\rangle^{1/2} , \tag{2.53}$$

$$|g_{k+1}\rangle = \beta_k^{-1} |s_k\rangle , \tag{2.54}$$

with the initial conditions $\beta_0 = 0$ and $|g_1\rangle = \langle\phi| V |\phi\rangle^{-1/2}$.

Chapter 3

Numerical results

3.1 Nyström method

The method introduced in the first section of the previous chapter was numerically tested on a potential of Malfliet-Tjon type used broadly in low-energy nuclear physics, namely

$$V(r) = V_R \frac{e^{-\mu_R r}}{r} - V_A \frac{e^{-\mu_A r}}{r}. \tag{3.1}$$

Simple integration gives for the matrix elements of V in the momentum representation

$$V(\vec{q}', \vec{q}) = \frac{1}{2\pi^2} \left(\frac{V_R}{(\vec{q}' - \vec{q})^2 + \mu_R^2} - \frac{V_A}{(\vec{q}' - \vec{q})^2 + \mu_A^2} \right). \tag{3.2}$$

In this case, the integration intimated in the equation (2.3) can be carried out analytically with the result

$$v(q', q, x', x) = \frac{1}{\pi} \left[\frac{V_R}{\sqrt{(q'^2 + q^2 - 2q'qx'x + \mu_R^2)^2 - 4q'^2q^2(1 - x'^2)(1 - x^2)}} \right.$$
$$\left. - \frac{V_A}{\sqrt{(q'^2 + q^2 - 2q'qx'x + \mu_A^2)^2 - 4q'^2q^2(1 - x'^2)(1 - x^2)}} \right]. \tag{3.3}$$

The properties of the potential are determined by the four coefficients μ_R, μ_A, V_R, V_A. In the first part of our numerical tests the values given in the table 3.1 have been used.[1] Similar calculations using the same type of potential are performed in [4]. So as to compare our results, we decided to run our numerical tests with the same configurations as in this work.

As already mentioned in the introduction, the LS equation is treated in momentum space, the singularity present due to the free propagator is handled via

[1] in this section we use units such that $\hbar c = 197.3286$ Mev $\cdot$ fm $= 1$

V_A	μ_A [MeV]	V_R	μ_R [MeV]
3.1769	305.86	7.291	613.69

Table 3.1: Parameters of the potential

the identity (2.5). A suitable mapping (2.7) of the radial part of the momentum is applied and finally, the whole equation is discretized using Gauss-Legendre quadrature rule. Thus a matrix equation is obtained, which is then solved by means of pivoted LU decomposition. When we denote the count of mesh points for the q'' variable as N_q and the same quantity for the x'' variable as N_x, then the expected time complexity should be $\mathcal{O}(N_q^3 N_x^3)$, because the matrix experiencing the LU decomposition is in general not sparse.

As a first numerical test of this method, we tried to calculate for several values of the energy the angular dependency of the on-shell T-matrix element $T(q_0, q_0, x)$, where x denotes the cosine of the scattering angle. The calculation for each energy was performed with increasing size of the grid in order to test whether the convergence is achieved.

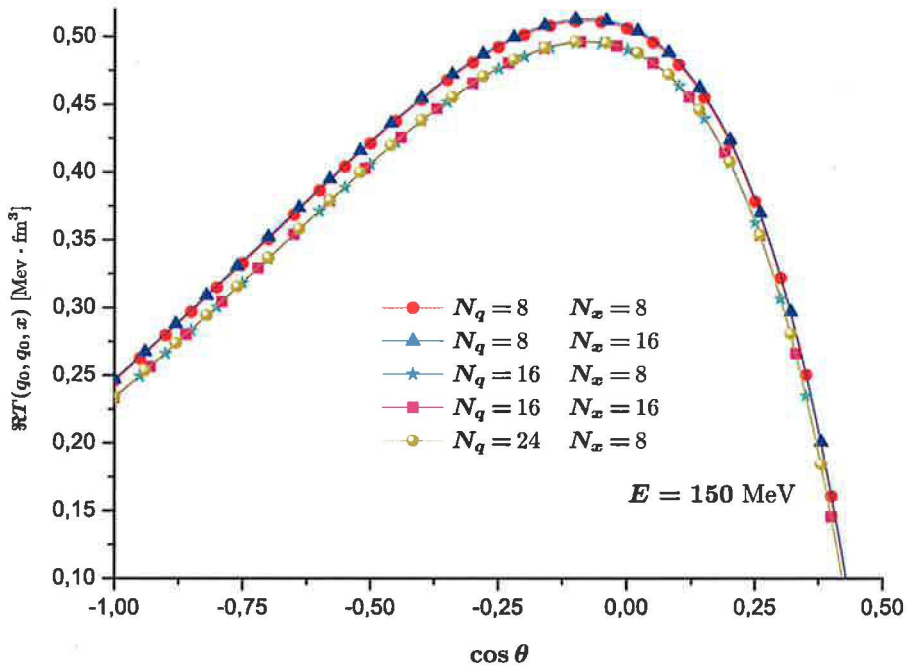

Figure 3.1: Angular dependency of $\Re T(q_0, q_0, cos\theta)$ for $E = q_0^2 = 150\,\mathrm{MeV}$

To testify our results we have also performed the partial wave decomposition and examined consequently, how much partial waves are needed to describe the scattering process properly. The quantity $T(q_0, q_0, x)$ can be expanded into partial

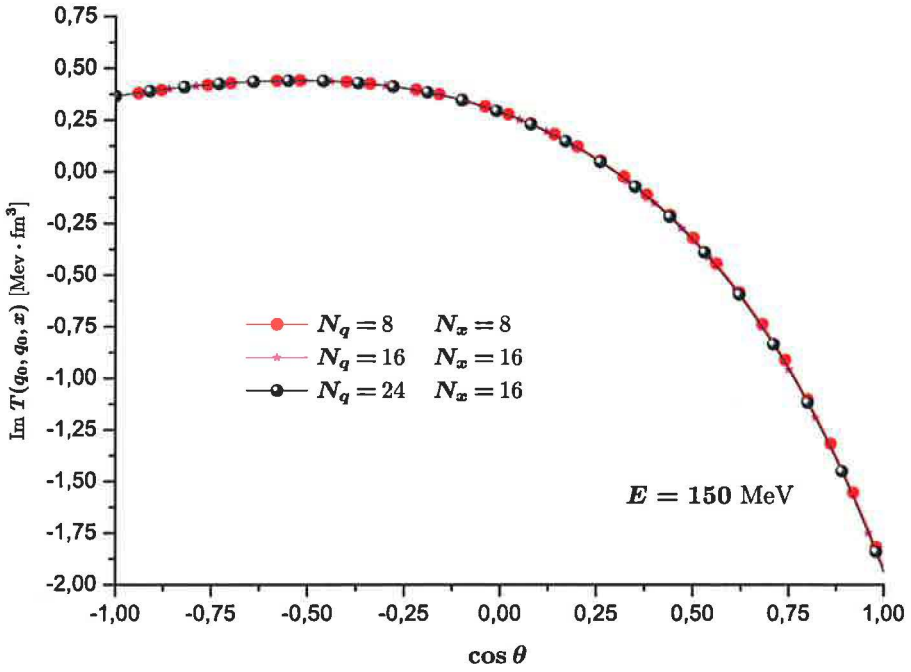

Figure 3.2: Angular dependency of Im $T(q_0, q_0, cos\theta)$ for $E = q_0^2 = 150\,\mathrm{MeV}$

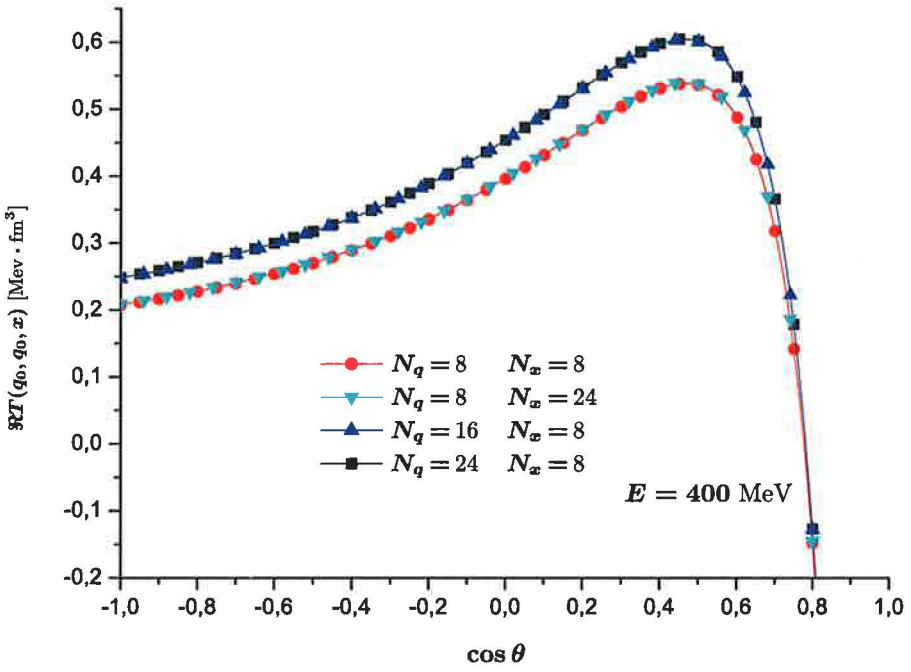

Figure 3.3: Angular dependency of $\Re T(q_0, q_0, cos\theta)$ for $E = q_0^2 = 400\,\mathrm{MeV}$

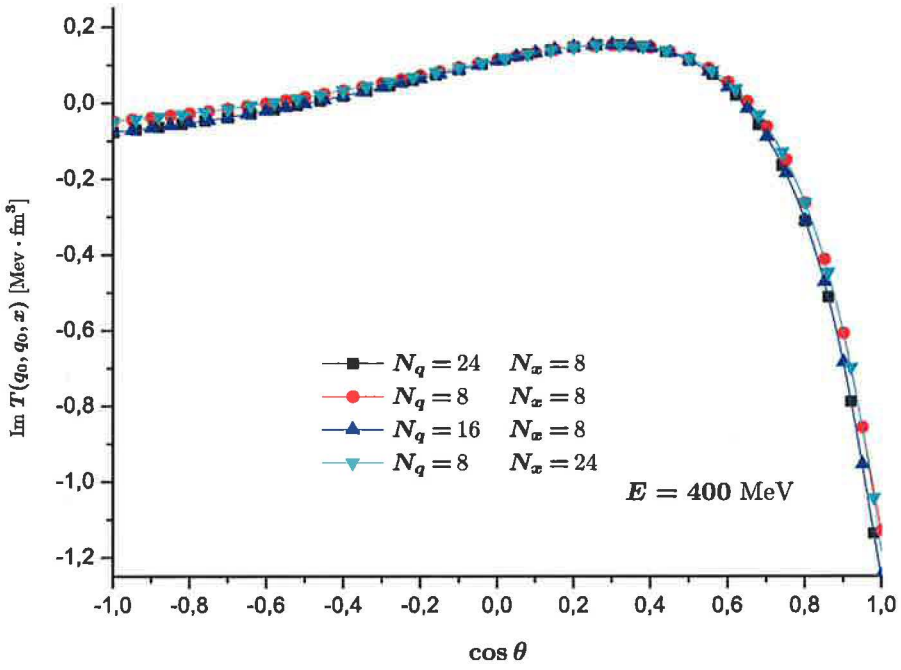

Figure 3.4: Angular dependency of Im $T(q_0, q_0, cos\theta)$ for $E = q_0^2 = 400\,\mathrm{MeV}$

waves in standard manner by means of the following equation as

$$T(q_0, q_0, x) = \sum_{l=0}^{\infty} \frac{2l+1}{4\pi} T_l(q_0) P_l(x), \tag{3.4}$$

where

$$T_l(q_0) = \frac{2}{\pi} \frac{1}{q_0 m} e^{i\delta_l(q_0)} \sin \delta_l(q_0). \tag{3.5}$$

The quantity $\delta_l(q_0)$ denotes the phase shift for given angular momentum l. Its determination was in our calculations based on direct integration of the radial Schrödinger equation and subsequent examination of the asymptotic behavior of the found solution. The integration itself was based on the well known Numerov two step fifth order method and Cash Raptis two step sixth order method. The usage of two methods with different order of accuracy makes it possible to estimate the global error of the constructed solution. For if we denote the solution in $n-$th step obtained by means of the Numerov method as y_n^N and its sixth order counterpart as y_n^C, then the difference $y_n^N - y_n^C$ can be taken as an estimate for the global error, according to which the integration step size can be properly adjusted. The knowledge of this quantity allows us so to implement a heuristic step size controlled integration algorithm. Details can be found in the Appendix B. Obtained results are depicted in graphs 3.5, 3.6, 3.7 and 3.8.

More thorough look on the equation (3.5) reveals, that the imaginary part of the on-shell T-matrix needs less partial waves to describe its behavior. Indeed,

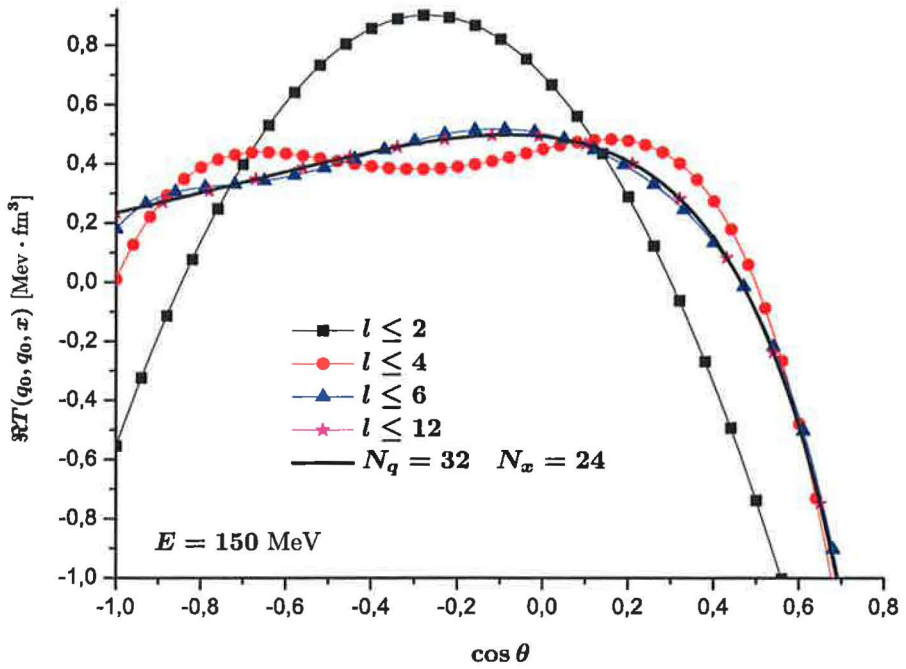

Figure 3.5: Angular dependency of $\Re T(q_0, q_0, cos\theta)$ for $E = q_0^2 = 150\,\mathrm{MeV}$

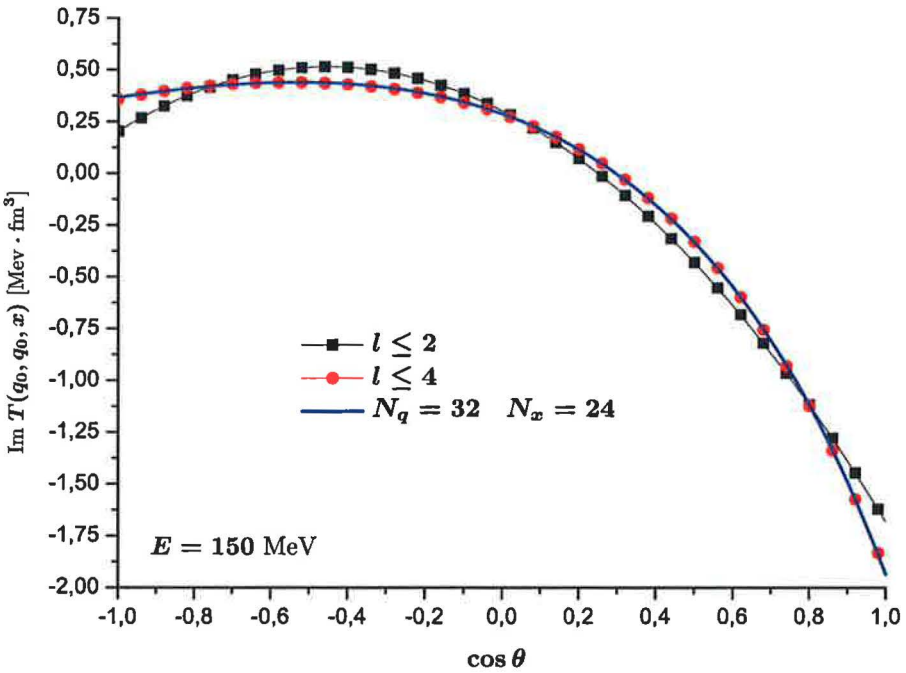

Figure 3.6: Angular dependency of Im $T(q_0, q_0, cos\theta)$ for $E = q_0^2 = 150\,\mathrm{MeV}$

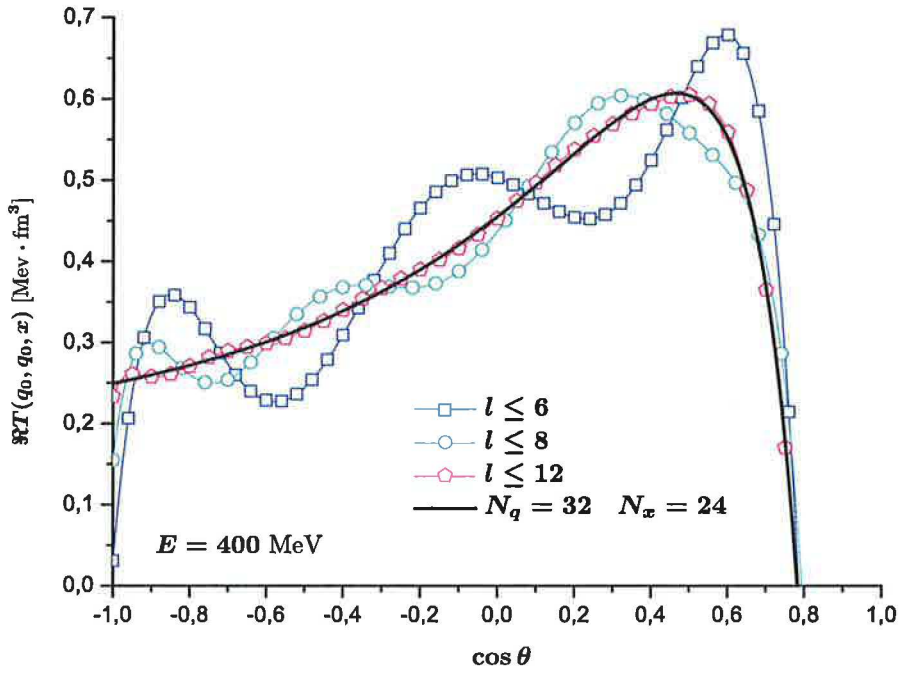

Figure 3.7: Angular dependency of $\Re T(q_0, q_0, cos\theta)$ for $E = q_0^2 = 400\,\mathrm{MeV}$

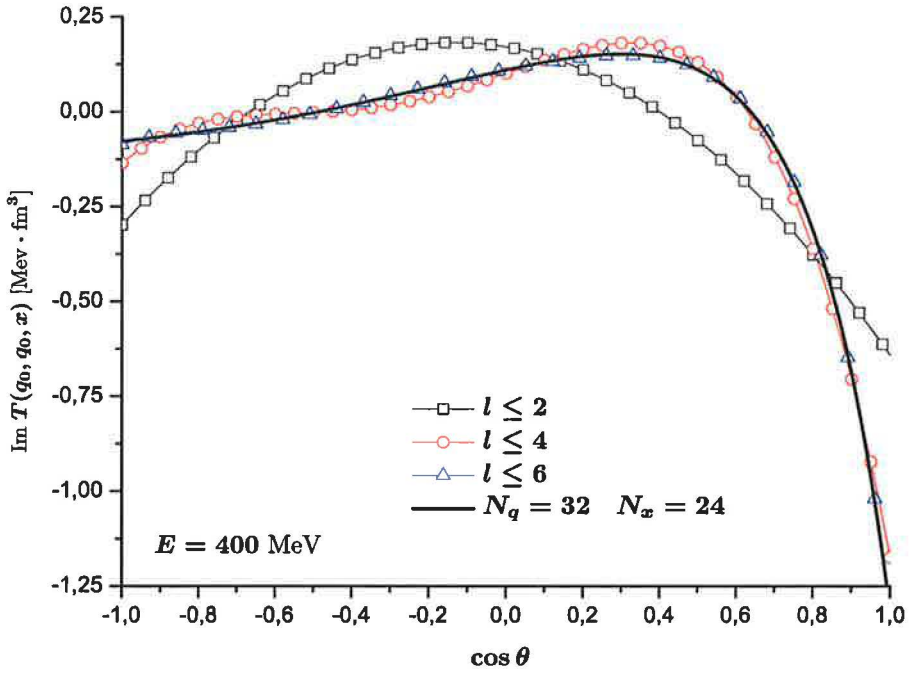

Figure 3.8: Angular dependency of Im $T(q_0, q_0, cos\theta)$ for $E = q_0^2 = 400\,\mathrm{MeV}$

the real part of the quantity $T_l(q_0)$ introduced in equation (3.5) is proportional to $\sin 2\delta_l$, whereas the imaginary part is proportional to $\sin^2 \delta_l$. For higher angular momenta, the phase shift will tend to zero, so the real part will decrease as δ_l and the imaginary part as δ_l^2. The situation is slightly more complicated for higher energies because of the anticipated presence of a relatively strong peak in forward direction making the description by means of partial waves more difficult.

According to [4], the potential under consideration should for $V_A = 5.4$ show a resonance $E_{res} = 0.9267 - i0.1821$ for $l = 1$, i.e. in the $p-$wave. We have computed the angular and energy dependence of the differential scattering cross section in order to test how this method copes with such phenomena. Because the pole of the T-matrix is near to real axis and also near the origin, some accuracy complications could be expected because of above mentioned reasons.

Nevertheless, the obtained dependency depicted in the figure 3.9 shows more or less the expected behavior. In order to quantify the resonance more precisely, we have plotted the energy dependency only of the contribution of the p-wave to the total T-matrix element together with a cut of previous graph for $\cos\phi = -1$ and performed a fit with the formula for the Fano shape resonance, i.e.

$$f(E) \approx \frac{(q\Gamma_{res}/2 + E - E_{res})^2}{(E - E_{res})^2 + (\Gamma_{res}/2)^2}. \tag{3.6}$$

The numerical values of the obtained parameters are summarized in the table 3.2.

q	E_{res} [MeV]	Γ [MeV]
5.160	0.975	0.392

Table 3.2: Computed parameters of the Fano shape resonance

The final plot is depicted in figure 3.10. In accordance with our previous assumption, the p-wave contribution to the total T-matrix is dominant in the resonant energy region.

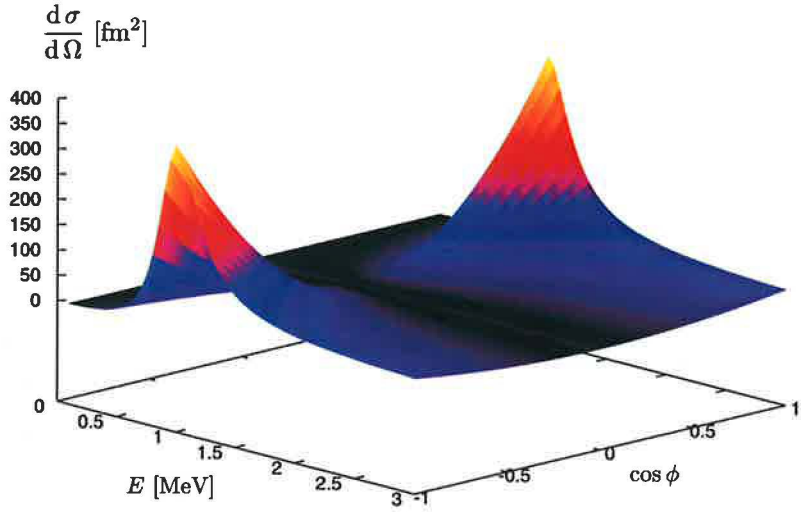

Figure 3.9: Angular and energy dependency of the differential cross section for $V_A = 5.4$.

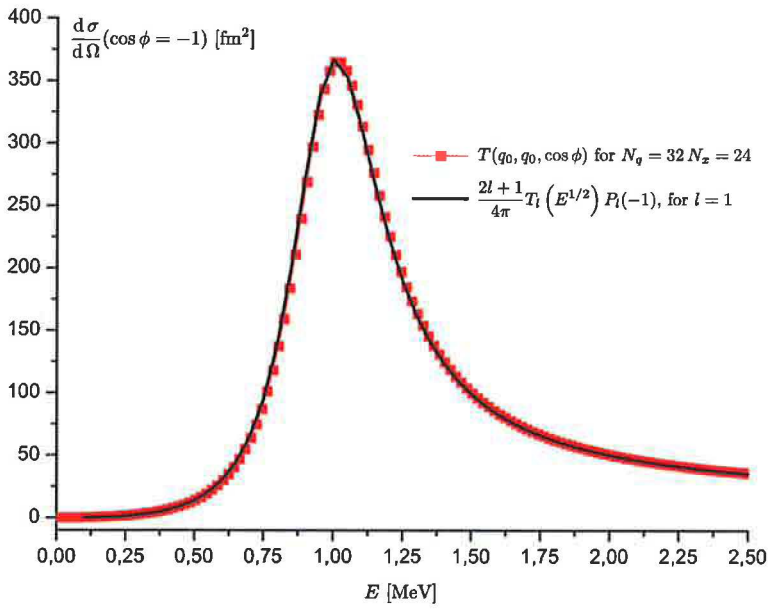

Figure 3.10: Energy dependency of the differential cross section for $V_A = 5.4$ and $\cos\phi = -1$.

3.2 Nyström-Chebyshev method

In order to test the numerical properties of this method, we performed similar calculations as in the previous section, so as to compare consequently the obtained results. Again, the local interaction was supposed to correspond to a potential of the Malfliet-Tjon type (3.1). Since the singularity in the kernel of the corresponding integral equation is handled more precisely than in the Nyström method, we anticipate, that this approach should be superior to the former method.

Several questions arise naturally concerning the convergence and accuracy of this method. In fact, we have three main free parameters, which could affect these properties. Namely the count of mesh points in the angular variable N_x, the count of the Chebyshev terms N in the expansion (2.14) and the count M of Chebyshev nodes used by the quadrature rule (2.17). Concerning the integral over the angular variable x, the situation is very similar to the Nyström method, so the main improvement is to be awaited in the integration over the radial part of momentum (i.e. over the variable y after performing the nonlinear transformation (2.10)).

It should be noted, that the substitution (2.10) depends on a real parameter C, which hasn't been discussed so far. Its value should be from the theoretical point of view completely arbitrary (except zero, of course). However, in this work, we made use of a special choice of C, namely $C = q_0$. This choice has several consequences. The most apparent one is probably the fact, that the incoming momentum q_0 maps according the transformation rule (2.10) onto 0, i.e. $y_0 \equiv y(q_0) = 0$. Further, the nodes of the quadrature rule used to approximate the integral over the variable y are given by (2.17). From this relation, we see, that if we choose simultaneously M to be even then for all $i = 1 \dots M$ the mesh points y_i are separated from the "singular" point 0 (i.e. we can be sure, that $y_i \neq 0$ for all $i = 1 \dots M$). Otherwise, i.e. if M would be odd, some i_0 in the range $1 \dots M$ would exist for which the corresponding y_{i_0} would be equal to 0 and thus it would coincide with y_0 making the set of equations (2.19) close to singular. Because of this reason, we choose $C = q_0$ and even M in all subsequent calculations based on the presented method.

The significance of the above mentioned parameter N lies in the way, how accurate the expression (2.15) is approximated by means of Chebyshev polynomials of the first kind. For some value of N, the expression $F(y', y'', x', x'')T(y'', y, x'')$ understood as a function of y'' behaves then effectively in our approximation as an ordinary polynomial of degree N multiplied by the weight function $(1-y'')^{-1/2}$. In order to calculate the expansion coefficients a_n, we need to evaluate numerically the defining integral (2.15). But if the approximation induced by a specific choice of N

is relevant, then the integrand actually reduces to a product of two polynomials of maximal degree N multiplied by the weight function $(1-y'')^{-1/2}$. The quadrature rule (2.17) used to cope with this task is of Gauss type and hence it has a degree of $2M-1$ for M mesh points. Therefore we expect, that if the approximation (2.15) turns out to be relevant then M should be set approximately equal to N in order to achieve maximal numerical precision, because higher values of M in the framework of the approximation (2.15) for some N can't increase in principle the precision of our calculations. Actually the effect of enormous value of M would be opposite because of unwanted rounding errors.

We performed several calculations to validate the above mentioned assumptions. The strategy of these tests is following. For a fixed value of N_x we have varied independently the values of the two remaining parameters M, N and consequently examined how this process affects the obtained value of the total cross section, which served us in these tests as a reference quantity characterizing the scattering process under investigation.

The following graph 3.11 depicts the dependency of the total scattering cross section on the value of the parameter N (the count of Chebyshev terms in the approximation (2.15)) for fixed value of M and N_x. The values of M are also depicted in the mentioned graph while N_x has been set to 24. (This value has been chosen on the basis of experiences with the Nyström method, in the framework of which this value turned out to be sufficient. Moreover, the integration over the angular variable is almost identical for both methods and so we expect the same behavior concerning the convergence and accuracy.)

A fleeting glance on the graph 3.11 justifies heuristically our assumptions. Indeed, the plateau of the values of σ is achieved approximately for $M \approx N$ as anticipated. On the basis of this ascertainment we assume in subsequent calculations in this chapter that the mentioned relation between the parameters M and N holds.

As already mentioned, an useful quantity, on which the convergence properties could be tested, is the total cross section of the scattering process under consideration. With N_x set again to 24, we have varied the parameter M and observed how this procedure affects the value of the total cross section. In order to compare the obtained numerical results with the Nyström method, we plotted the corresponding dependency into the apt graphs. So for example, the "x-variable" in the graph 3.12 has for the dependency labeled as "Nyström method" the meaning of the parameter N_q introduced also in the previous section while it is equivalent to the parameter M for the second dependency labeled as "Nyström-Chebyshev method". We performed these calculations for two values of energy, namely for $E = 400$ MeV and $E = 150$ MeV. The results are summarized in the graph 3.12

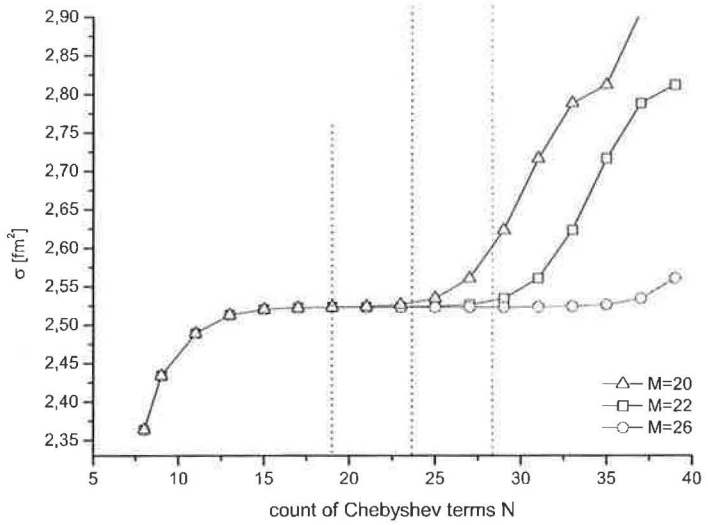

Figure 3.11: Dependency of σ on N for fixed M and $N_x = 24$ for $E = q_0^2 = 400\,\mathrm{MeV}$

and graph 3.13.

We clearly see the superiority of the presented method to the previous one especially for lower counts of mesh points in the radial part of the momentum. This behavior corresponds to our expectations because of the preciser approach to handle the integral singularity.

Up to now, we have considered the parameter N_x as fixed, because no singular behavior should be expected in the integration over the angular part. Nevertheless, the question of influence of this quantity on the convergence of the presented method should not remain unanswered. To this end, we depicted the dependency of the total scattering cross section on the two parameters N_x and M in the graph 3.14. Although the convergence is not monotone, we see, that the value of the total cross section can be obtained by means of this method with the accuracy of 5 decimal places for reasonable values of the parameters M and N_x. The second graph 3.15 depicts the corresponding dependency for the ordinary Nyström method. We see again, that our assumptions concerning the numerical performance of the presented method are justified, for the accuracy of the Nyström method in the same region of parameters space is at least by 1 decimal place lower.

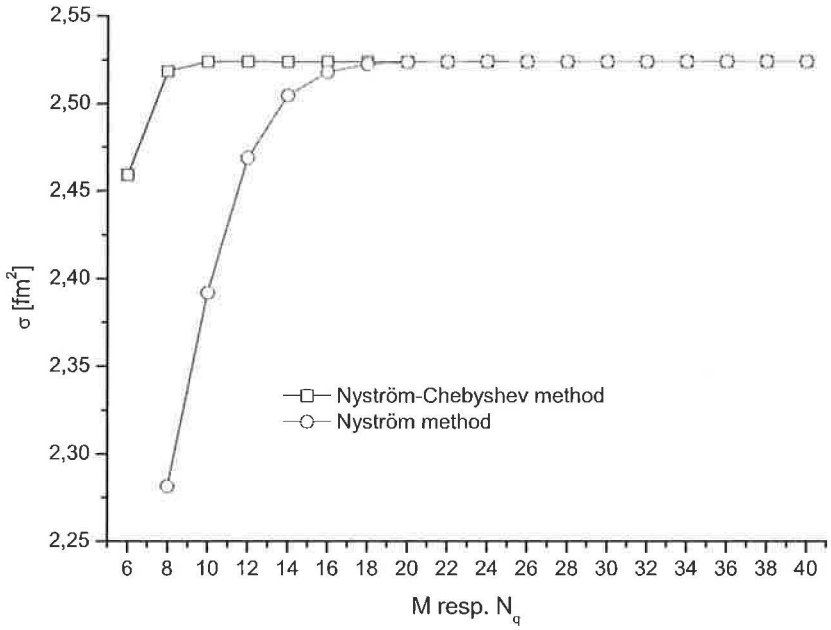

Figure 3.12: Convergence of the scattering cross section for $E = 400\,\mathrm{MeV}$

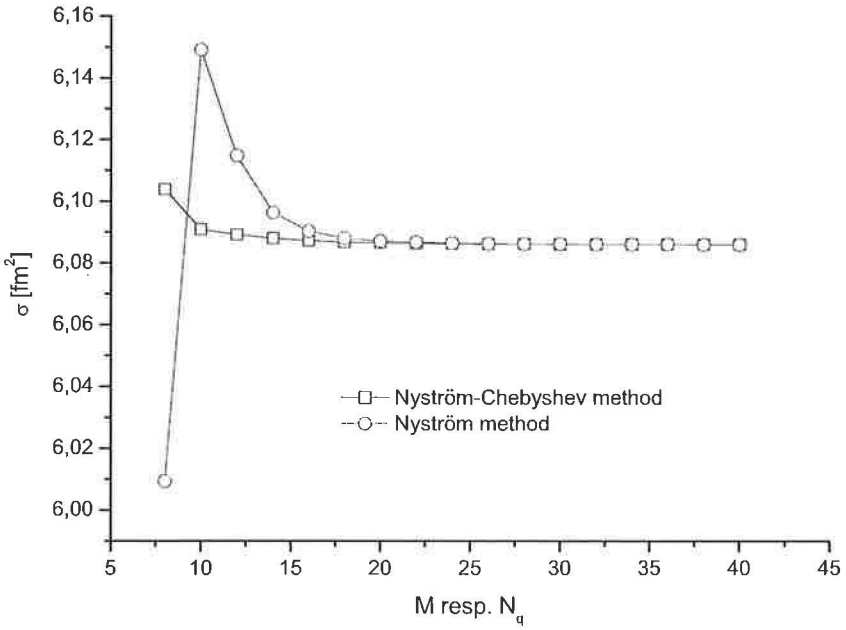

Figure 3.13: Convergence of the scattering cross section for $E = 150\,\mathrm{MeV}$

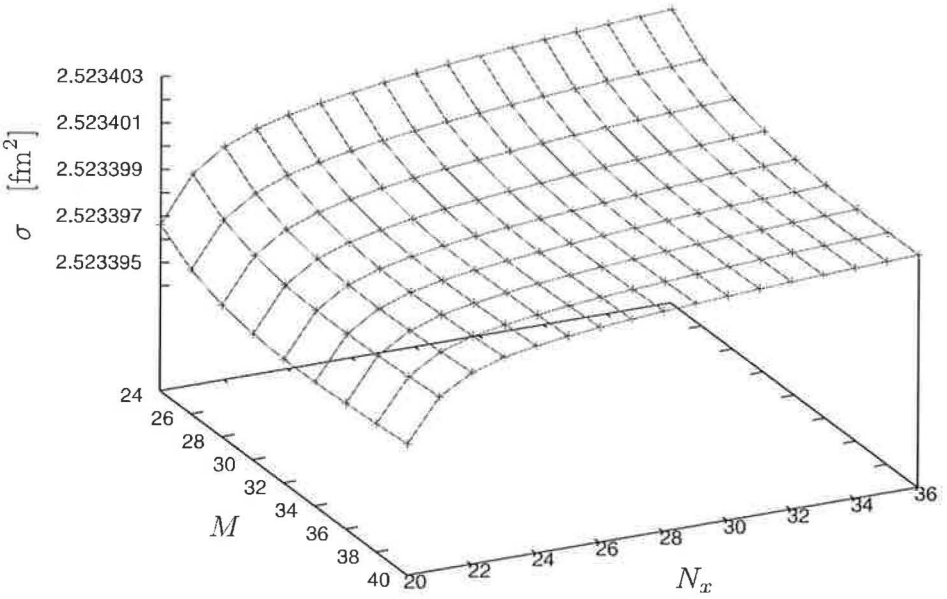

Figure 3.14: Convergence of σ for $E = 400\,\mathrm{MeV}$ for the Nyström-Chebyshev method

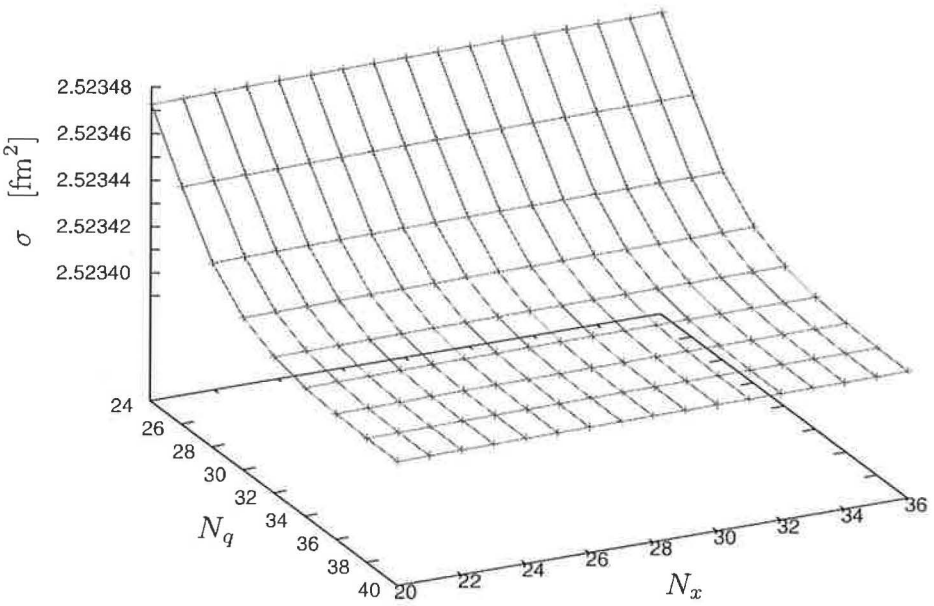

Figure 3.15: Convergence of σ for $E = 400\,\mathrm{MeV}$ for the Nyström method

3.3 R-matrix and Lanczos method

The numerical tests of the R-matrix method combined with Lanczos iterations consist in the calculation of the s-wave phase shift for scattering of an electron from the ground-state of a hydrogen atom in the presence of exchange terms, both for the singlet $\delta^{(+)}$ and triplet $\delta^{(-)}$ state. We choosed this model as our subject of interest in this section because similar calculations using different approaches can be found in the literature [20] offering the possibility to compare the results.

For the s-wave, the scattering problem reduces to solving the integral equation for the radial part of the corresponding partial wave. Namely[1]

$$\left(\frac{\mathrm{d}^2}{\mathrm{d}\,r^2} + k^2\right) R_0(r) = V(r)R_0(r) \pm \int_0^\infty K(r,r')R_0(r')\,\mathrm{d}r', \tag{3.7}$$

where in the case of electron hydrogen scattering

$$V(r) = -2re^{-2r}\left(1 + \frac{1}{r}\right) \tag{3.8}$$

$$K(r,r') = 2v(r)u(r') + \gamma u(r)u(r') \text{ for } r' < r \tag{3.9}$$

$$K(r,r') = 2u(r)v(r') + \gamma u(r)u(r') \text{ for } r' > r, \tag{3.10}$$

where following notation has been used

$$\begin{aligned} \gamma &= -k^2 - 1 \\ u(r) &= 2re^{-r} \\ v(r) &= \frac{u(r)}{r} = 2e^{-r}. \end{aligned}$$

The calculations are done with the method described in the last section of the previous chapter (let's denote it as RLS for further reference) and compared to results obtained with the other methods under consideration described briefly below.

- **S-IEM** is an spectral (that means, that the convergence with the increasing number of mesh points n is under some assumptions faster than $\mathcal{O}(n^{-p})$ for arbitrary $p \in \mathcal{N}$) integral equation method developed recently by G. H. Rawitscher et. al. The original work [20] introduces a new method for solving LS equation with local potentials. Nevertheless, they have managed to develop [5] a generalization which is able to handle properly the nonlocal

[1] The kernel $K(r,r')$ in the equation (3.7) above can be equivalently restated in a slightly modified way as $K(r,r') = u(r)u(r')\,(\gamma + 2/r_>)$, where the usual symbol $r_>$ stands for r or r' according to which quantity is bigger.

terms, which can be expressed in the special form (3.9). The LS equation for the s-wave can be with suitable normalization schematically written in concise form as $(I + K)\psi(x) = \sin(kx)$. Further, the integration range is divided into several subsectors. In [5], it is nicely shown, that the final solution on each of the subintervals can be found as linear combination of four functions, which can be obtained by acting of the inverse of $(I + K_i)$ on four different "source" terms, where K_i denotes the restriction of K on the $i-$th subinterval. These source terms are equal for each subsector and are determined by the very nature of the potential. The original problem is then reduced to solving a set of linear equations for the coefficients in the linear combinations on each subinterval. Practical details can be found in [5] and [20].

- **M-IEM** is an iterative method originally introduced by B. T. Kim and T. Udagawa in [13]. Roughly speaking, the core of this method relies on utilizing of the Lanczos iterations for the complete LS equation. The authors use some additional computational improvements (they add a relatively arbitrary term to the local potential which is then again subtracted from the non locality), which should reputedly improve the rate of convergence. Nevertheless they don't discuss effects of this approach in detail and we haven't pursuited this issue further.

- **N-IEM** stands for an older non iterative integral equation method based on the work by W. N. Sams and D. J. Kouri [21]. In principle, the final solution of the original one channel LS equation is expressed formally as a linear combination of two terms. The coefficients in this linear combination are profitably chosen (a linear set of two equations is to be solved to ensure this property) so that each of the two terms satisfies a Volterra integral equation of the second kind, which is then handled by standard means using e.g. trapezoidal quadrature rule. Once we have solved these Volterra equations, we have to determine the two coefficients in the linear combination in the expansion of the original solution. As already mentioned, they are required to satisfy a system of linear equations with coefficients which are obtained in the first step of this method. The general discussion and a slight generalization of this method can be found in [21].

  We give here only a brief description of application of this method to the above mentioned problem of s–wave scattering in Hartree–Fock aproximation. If we denote the sought wave function as $\psi(r)$ then the corresponding differential equation can be written according to the footnote on the page

30 as

$$\left[\frac{\mathrm{d}^2}{\mathrm{d}r^2} + 2(1+\frac{1}{r})e^{-2r} + k^2\right]\psi(r) = \mp\Big(8\int_0^\infty r_>^{-1} r' e^{-r'}\psi(r')\,\mathrm{d}r' \qquad (3.11)$$
$$-4(1+k^2)\int_0^\infty r' e^{-r'}\psi(r')\,\mathrm{d}r'\Big) r e^{-r}.$$

The term containing $r_>$ is the eliminated by standard trick consisting in splitting the integral $\int_0^\infty$ to sum of two integrals $\int_0^r$ and $\int_r^\infty$. We can equivalently rewrite the differential equation (3.11) in the integral form (we use the real free particle Green function). After some manipulations we obtain

$$\begin{aligned}\psi(r) =& \sin(kr) - \frac{1}{k}\cos(kr)\int_0^r G(r')\sin(kr')\,\mathrm{d}r' \\ &+ \frac{1}{k}\sin(kr)\int_0^r G(r')\cos(kr')\,\mathrm{d}r' - \frac{1}{k}\sin(kr)\int_0^\infty G(r')\cos(kr')\,\mathrm{d}r' \\ &\mp \frac{4B}{k}\int_0^\infty \sin(kr_<)\cos(kr_>) r' e^{-r'}\,\mathrm{d}r',\end{aligned} \qquad (3.12)$$

where B is a linear functional of the final solution $\psi(r)$ and can be expressed as

$$B\left[\psi(r)\right] \stackrel{\text{def}}{=} 2\int_0^\infty e^{-r}\psi(r)\,\mathrm{d}r - (1+k^2)\int_0^\infty r e^{-r}\psi(r)\,\mathrm{d}r, \qquad (3.13)$$

while $G(r)$ is a function of the radial variable r depending also linearly in a functional sense on the solution $\psi(r)$. Namely

$$G(r) \stackrel{\text{def}}{=} 2(1+\frac{1}{r})e^{-r}\psi(r) \pm 8\left(\int_0^r r' e^{-r'}\psi(r')\,\mathrm{d}r' - r\int_0^r e^{-r'}\psi(r')\,\mathrm{d}r'\right) e^{-r}. \qquad (3.14)$$

We now define $\psi_0(r)$ to be the solution of the homogeneous part of the integral equation (3.12). Explicitly written

$$\begin{aligned}\psi_0(r) = \sin(kr) &- \frac{1}{k}\cos(kr)\int_0^r G_0(r')\sin(kr')\,\mathrm{d}r' \\ &+ \frac{1}{k}\sin(kr)\int_0^r G_0(r')\cos(kr')\,\mathrm{d}r'.\end{aligned} \qquad (3.15)$$

Consequently we seek the original solution in the form of a linear combination of the solution of the homogeneous equation ψ_0 and a "correction" ψ_2. Namely $\psi(r) = (1+C)\psi_0(r) + D\psi_2(r)$, where C and D are yet undetermined c–numbers. Substituting this expression into equation (3.12) and utilizing the fact, that ψ_0 is by definition a solution of the homogeneous equation,

gives for $\psi_{1,2}$ the following formula

$$\begin{aligned} C\psi_0(r) + D\psi_2(r) = &- \frac{1}{k}\cos(kr)\int_0^r \sin(kr')\left[CG_0(r') + DG_2(r')\right]\mathrm{d}r' \\ &+ \frac{1}{k}\sin(kr)\int_0^r \cos(kr')\left[CG_0(r') + DG_2(r')\right]\mathrm{d}r' \\ &- \frac{1}{k}\sin(kr)\int_0^\infty \cos(kr')\left[(1+C)G_0(r') + DG_2(r')\right]\mathrm{d}r' \\ &\mp \frac{4}{k}(CB_0 + DB_2)\int_0^\infty \sin(kr_<)\cos(kr_>)r'e^{-r'}\,\mathrm{d}r'. \end{aligned} \tag{3.16}$$

Further, we can fix the coefficients C, D by requiring

$$\begin{aligned} D &= CB_0 + DB_2 \\ C &= -\frac{1}{k}\int_0^\infty \cos(kr')\left[(1+C)G_0(r') + DG_2(r')\right]\mathrm{d}r'. \end{aligned} \tag{3.17}$$

As a consequence of this choice all terms in the equation (3.16) concerning the function $\psi_0(r)$ drop out and we become a formula determining solely $\psi_2(r)$. Concretely

$$\begin{aligned} \psi_2(r) = &\mp \frac{4}{k}\int_0^\infty \sin(kr_<)\cos(kr_>)r'e^{-r'}\,\mathrm{d}r' + \\ &- \frac{\cos(kr)}{k}\int_0^r G_2(r')\sin(kr')\,\mathrm{d}r' + \frac{\sin(kr)}{k}\int_0^r G_2(r')\cos(kr')\,\mathrm{d}r'. \end{aligned} \tag{3.18}$$

Thus the strategy is as follows. We can solve the Volterra integral equations (3.15), (3.18) by standard means, because only the knowledge of $\psi_{0,2}(r)$ at previous grid points is needed for the computation of "next" value of these functions. Once we have obtained $\psi_0(r)$ and $\psi_2(r)$, we can easily calculate the coefficients B_0 resp. B_2 and consequently solve the two linear equations for C and D obtaining thus the complete solution of the original problem.

- **MCFV** is an iterative method based on series of papers [8], [9] and [10] by J. Horáček and T. Sasakawa. In this approach the local and nonlocal parts of the complete potential are also handled separately as in the RLS method. Nevertheless, the Green's function is constructed in this case directly from the two independent solutions of the free Schrödinger equation. This procedure seems to be less numerically accurate than the R-matrix machinery, especially in the classically forbidden region, where the difference in the order of magnitude of the two independent solutions is considerable. The nonlocal part is then handled iteratively by successive subtractions of

separable terms from the potential, until it is week enough, so as to the remaining term can be neglected. Moreover, the trapezoidal rule used in this method allows to incorporate the Romberg extrapolation scheme, which is a handy tool suitable to improve the overall accuracy of the entire method. The implementation details can be found in [7].

As mentioned in the theoretical introduction, the RLS method firstly divides the integration range into several sectors and then builds a orthonormal basis on each of them. The basis functions are defined by the equation on eigenfunctions (2.26). The construction of this basis is the most time consuming part of the entire computation. If we denote the count of sectors as N_s and the count of basis functions on each sector as N_b, then the expected time complexity should be $\mathcal{O}(N_s N_b^3)$, because of the necessity to diagonalize the matrix representation of the operator $\bar{K} + V(r)$ N_s–times. However, this part of computation is the only energy dependent (the energy of the incoming electron is understood) element of the method. So it is possible to construct the basis once and then eventually reuse it, if a calculation for different energy is desired. This is very profitable feature of this method enabling fast computation of the phase shift dependence on energy as illustrated below. The measured time complexity of the presented method depicted in the

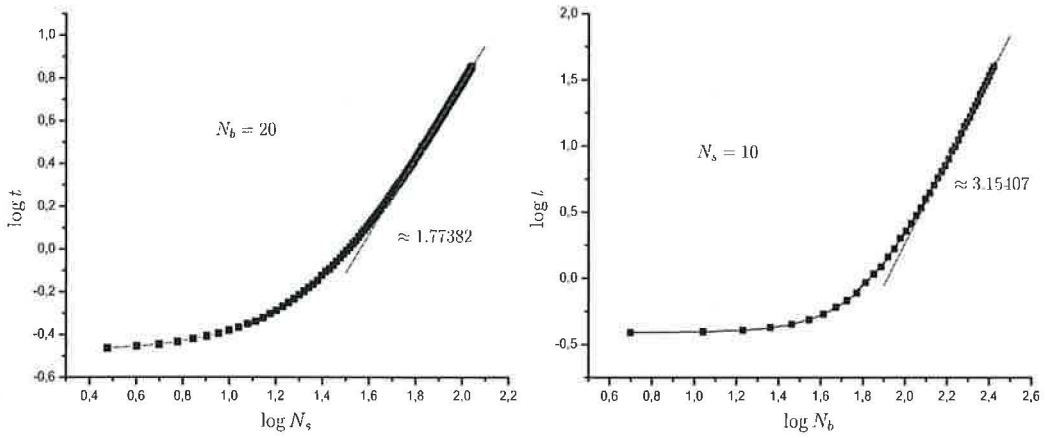

Figure 3.16: Measured time complexity of the presented method

figure 3.16 shows, that concerning the count of the basis functions per sector N_b, the asymptotic behavior is close to the expected, nevertheless the time grows with increasing count of sectors almost quadratically. This fact suggests, that the integration method used plays also an important role. Indeed, the theoretical time complexity of the composite Clenshaw-Curtis quadrature rule described in Appendix A for a direct implementation is expected to be quadratic in the count of the sectors. According to [12], the costs on this part of computation can be reduced to $\mathcal{O}(N_s \log(N_s))$, nevertheless we haven't pursuited this matter further.

Mainly because of the reason, that for typical calculations performed in this work, small count of sectors is needed, for which the asymptotic behavior doesn't play a vital role.

Although the implementation is relatively straightforward, we would like to point out some facts, that turned out to be crucial in light of the accuracy of the computation. In the first development phase we based the method on Gauss-Legendre quadrature. This choice would be adequate for smooth potential. But as can be easily seen, the potential (3.9) has a cusp (noncontinuous first derivatives) for $r = r'$. We have tested, whether this fact can be eventually neglected and how this omission would affect the total accuracy. It turns out, that with Gauss type quadrature, the usefulness of the method was very limited. The value $\delta^{(+)}$ was obtained only with 4–5 significant figures but only at the expense of extremely dense grid (cca. 200 mesh points per sector), high count of sectors ($N_s \approx 100$) and basis functions ($N_b \approx 100$). Needless to say, that the total time of computation also overreached the limits of propriety in this case.

These problems were surmounted by using another type of quadrature adopted from [12], suitable among others for kernels of the type (3.9). The details of this approach are briefly described in the appendices. For the purposes of this work the composite quadrature rule has been used (denoted as CC–quadrature for further reference). Incorporating this enhancement into the framework of the RLS method yielded indeed better accuracy, but the improvement was far from expected. It was managed to obtain the value $\delta^{(+)}$ only with 1–2 more significant figures than with ordinary Gauss–Legendre quadrature rule.

Some investigation showed, that the problem is buried in the fact, that $V(0+) = \infty$. Indeed, omitting the term $1/r$ in the local potential yielded accuracy close to the machine precision. It turned out, that the construction of the eigenfunctions of the operator $\tilde{K} + V(r)$ needed to be numerically improved. The basis on the first sector is constructed from a set of Jacobi polynomials ($P_i^{(0,2)}(r)$, where $i = 0, \cdots, N_b$). Because $P_i^{(0,2)}(0) = 0$, the first boundary condition (2.25) is automatically fulfilled. To determine the eigenfunctions, one needs to compute expressions of type $\int_0^R P_i^{(0,2)}(r) V(r) P_j^{(0,2)}(r)\,\mathrm{d}r$, where R is the length of the first sector. A first approach we have used to cope with this task was to use a temporary basis of eigenfunctions of the operator $\hat{r}$, in which these elements take a simple form, and then to use the inverse transformation. However, in the case that the potential grows to infinity at $r = 0$, this approach was unable to furnish the eigenvalues of $\tilde{K} + V(r)$ with sufficient accuracy. In this case, it turned out, that more reliable is to compute the mentioned matrix elements directly using Gauss-Legendre quadrature of higher order (typically $\approx N_b^2$) furnishing much better accuracy.

One could ask, whether this drawback of the method could be dispatched by using of denser grid where appropriate (typically the first sector) or by narrowing the sectors, where we are expecting some oddities. The mentioned narrowing

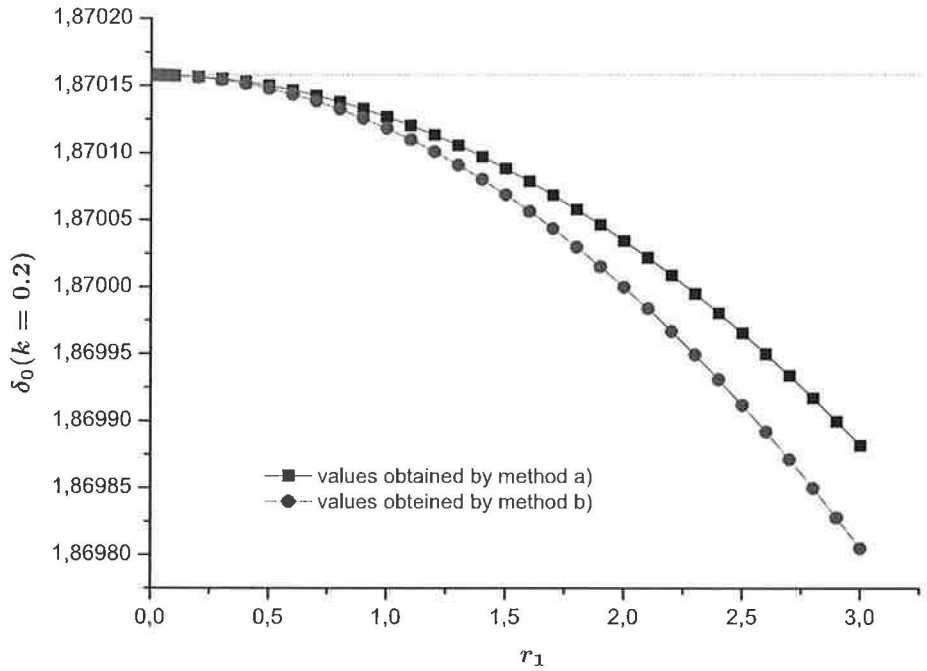

Figure 3.17: Influence of the width of the first sector

would also naturally improve the approximative properties of the constructed DVR basis on this sector. To illustrate this effect we have performed the following calculations.

An example of the influence of the first sector's width on the phase shift is depicted in picture 3.17. The quantity r_1 on the x-axis stands for the width of the first sector in atomic units. All calculations done to obtain this graph were performed with constant count of sectors and mesh points, namely $N_s = 6$, $N_b = 20$, $r_{max} = 20$ and 192 mesh points (i.e. 32 mesh points per sector). Moreover, two different approaches have been used to calculate the phase shift in this case. Although they coincide when the method converges, in this case they are yielding slightly different values. The former approach denoted as method a) in the picture calculates the T-matrix element by direct integration by means of the well-known two potential formula. The latter differs in the way how it handles the contribution from the local potential to the total phase shift. It is based on the equation (2.46), which is able to furnish the value of the logarithmic derivative on the edge of last sector. Armed with this knowledge we can then easily calculate the phase shift by some juggling with spherical Bessel functions on the base of knowledge of asymptotic behavior of the radial wave function. As can be seen from the mentioned picture, the "method" b) converges more slowly, so the inaccurately determined basis on the first sectors contaminated also the

accuracy obtained by the propagation formula (2.46).

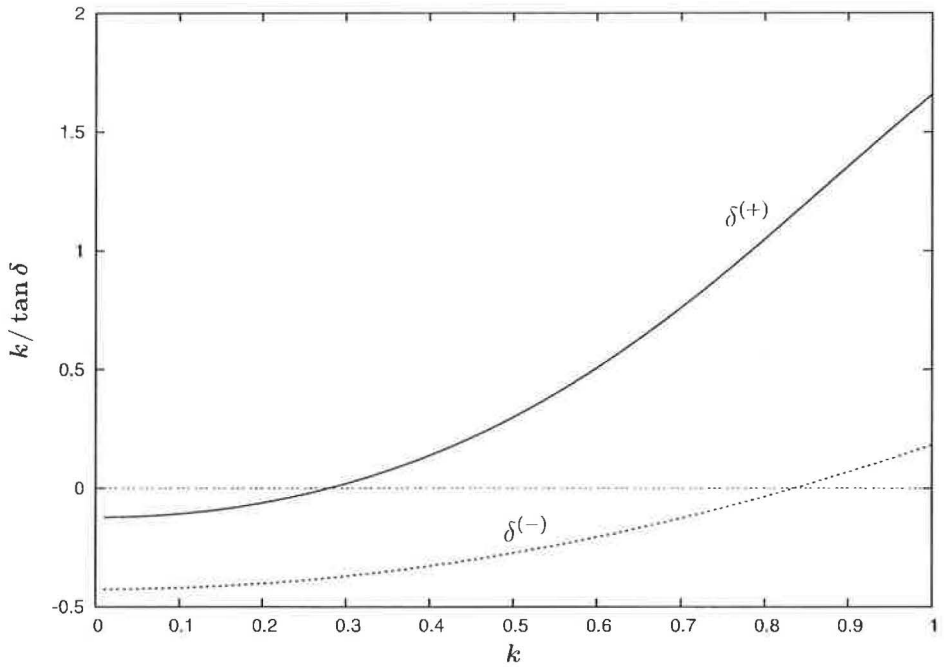

Figure 3.18: $\delta^{(\pm)}$ energy dependency

Relatively detailed accuracy study of the N-IEM method is obtained in [21], so we decided to test the method presented in this work for the same set of parameters. Results of the other mentioned methods for these parameters can be found in [5] and [7]. The case chosen is the singlet phase shift with exchange $\delta^{(+)}$. The magnitude of the wave number is $k = 0.2/a_0$, where a_0 is the Bohr radius ($a_0 = 1$ in atomic units), and the maximum radial distance (range of integration) is set to $20a_0$.

The results are summarized in the table 3.3. The number of significant figures in the first column is determined from the stability of the phase shift value after rounding, when compared to the result corresponding to higher count of mesh points.

method	$\delta^{(+)}$	no. of mesh points
RLS	1.870 157 88	64
S-IEM	1.870 157 9	80
MCFV	1.870 157 9	128
M-IEM	1.870 156	4000
N-IEM	1.870 15	4000

Table 3.3: Accuracy of $\delta^{(+)}$ for methods under investigation

More transparent overview of the convergence properties of these method is depicted in figure 3.19, in which we are dealing with "inverse" task, i.e. with determining the count of mesh points necessary to obtain some prescribed count of significant digits. As can be seen from this picture, the proposed RLS method

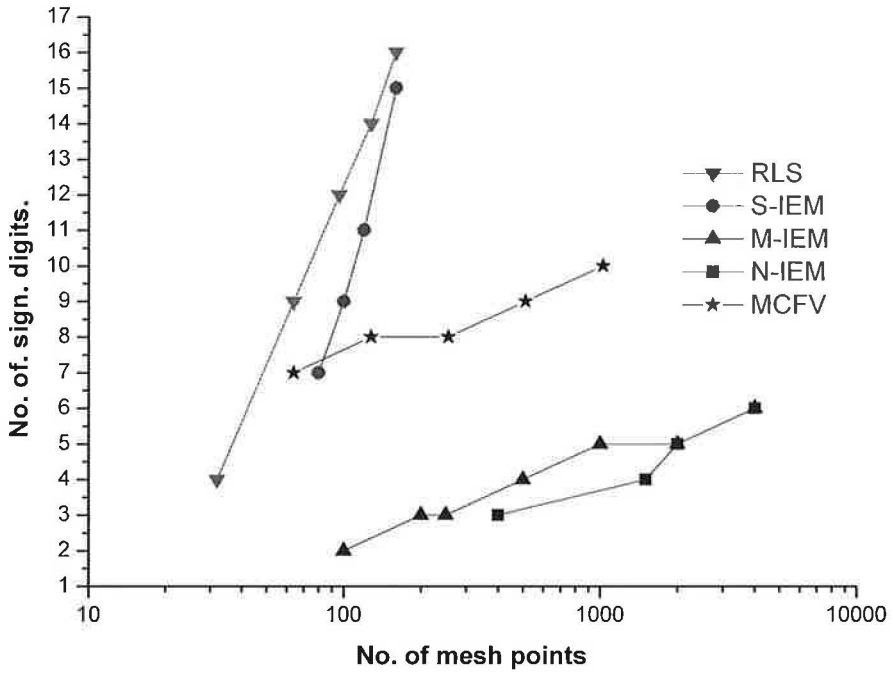

Figure 3.19: Accuracy comparison of tested methods

seems to be very stable even for low number of mesh points. We believe, that it is primarily thanks to the accurate construction of the Green's function via the R-matrix method.

Another issue worth mentioning concerns the tolerance in the Schwinger-Lanczos iteration algorithm, which is used to handle the nonlocal part of the potential. The dilemma is following. Either we choose the tolerance too generous and the obtained result will be affected by this omission, or we choose the tolerance too restrictive and if we don't restrict the maximum count of iterations, then the sought solution will be after a few steps kicked out from equilibrium by successive undesired iterations. With this matter in mind, one could naturally ask, how a tolerance (say Δt) would in computing the T-matrix element via Schwinger-Lanczos algorithm affect the accuracy of the total T-matrix element. As mentioned in the introduction, the problem of solving the complete LS equation $|\phi\rangle = |u\rangle + G_0(E)(V+W)\,|\phi\rangle$ is decomposed into two partial quests, namely to solving the equation $|\overline{u}\rangle = |u\rangle + G_0(E)V\,|\overline{u}\rangle$ and consequently on the basis of

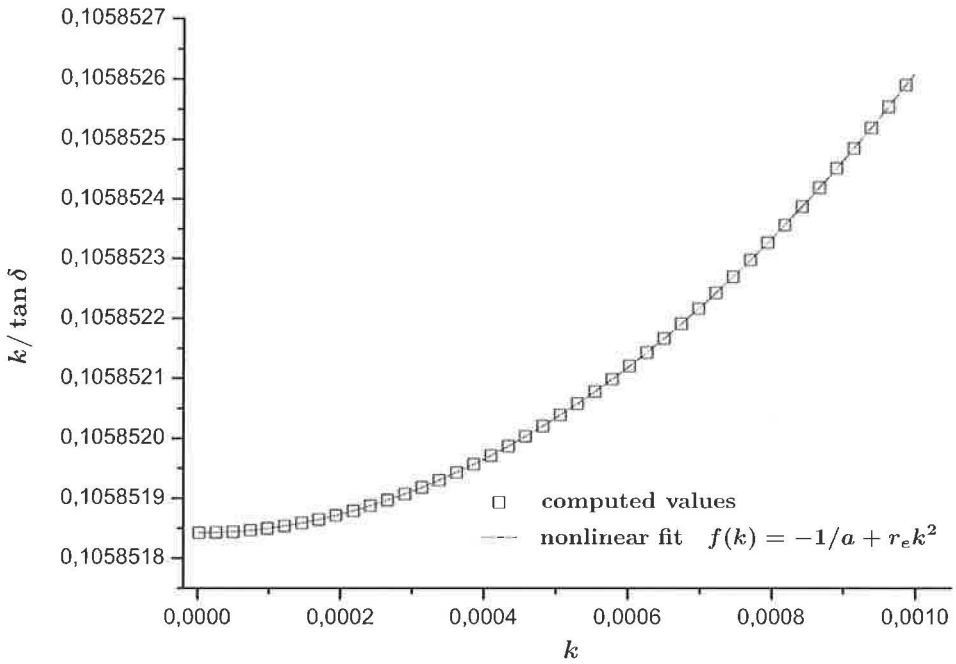

Figure 3.20: Effective range and scattering length... (singlet state)

knowledge of $|\overline{u}\rangle$ to solving of $|\overline{u}\rangle = |u\rangle + G_0(E)V\,|\overline{u}\rangle$. The total T-matrix element T is then given as $\langle u|\,V\,|\overline{u}\rangle + \langle\overline{u}|\,W\,|\phi\rangle$. If the ket $|u\rangle$ is normalized to $\delta(k-k')$, i.e. in the coordinate representation $\sqrt{2/\pi}krj_l(kr)$, then T is related to the desired phase shift as $\tan\delta_l = -\frac{\pi\mu}{2k}T$ (the reduced mass μ is supposed to be 1 in this work). So we have

$$\delta_l = \arctan(a - bt), \text{ where } a = -\frac{\pi\mu}{2k}\,\langle u|\,V\,|\overline{u}\rangle \text{ and } b = -\frac{\pi\mu}{2k},$$

where t is supplied by Schwinger-Lanczos iterations. Therefore, with fixed a a tolerance Δt in t will cause a discrepancy $\Delta\delta_l$ in the value δ_l equal to

$$|\Delta\delta_l| = \frac{b}{1 + (a - bt)^2}\,|\Delta t|\,.$$

For typical energies used during numerical tests in this work the quantities a, b and t are approximately equal to 1 and so is the coefficient standing before $\alpha \equiv |\Delta t|$ in the previous equation. However, the quantity b is inversely proportional to k, so for higher energies α will tend to zero allowing to increase the tolerance of the Schwinger-Lanczos algorithm. This behavior is what one would expect, because for higher energies and higher angular momenta, the particle is less influenced by the interaction.

As another application of the presented method, we tried to calculate the effective range r_e and scattering length a for the singlet state. These quantities

are defined by means of the power expansion of the expression $k \cot \delta_0$ in powers of k, namely

$$\frac{k}{\tan \delta_0} = -\frac{1}{a} + r_e k^2 + \mathcal{O}(k^3). \tag{3.19}$$

The results obtained for the singlet state case are depicted in the picture 3.20. As can be seen, good agreement with the asymptotic behavior has been achieved. The calculations for the values of the momentum k in the picture were performed for $r_{max} = 30$ a.u. with 6 sectors, 32 mesh points per sector and 20 basis functions per sector. The above mentioned parameters a, r_e were then obtained by standard Levenberg-Marquardt iteration algorithm for nonlinear fitting. Numerical values are in accordance with [5], although a different approach to determination of r_e and a has been used in this paper.

	r_e	a
singlet state	$1.51210 \pm 4.889 \cdot 10^{-9}$	$+8.10031 \pm 1.440 \cdot 10^{-10}$
triplet state	$0.61052 \pm 1.175 \cdot 10^{-8}$	$+2.34940 \pm 2.911 \cdot 10^{-14}$
no exchange	$0.76680 \pm 8.465 \cdot 10^{-9}$	$-9.44717 \pm 3.356 \cdot 10^{-13}$

Table 3.4: Effective range r_e and scattering length a for the s-wave

Chapter 4

Conclusion

In the present work, we have proposed several methods for treating the integral Lippmann–Schwinger equation both in the three as well as in the one dimensional case. Although the methods dealing with the three dimensional variant of LS equation were based on the assumption of local spin less "interaction", which reduces the dimension of the integral equation under consideration by one, the generalization to the more general case should be performed in a rather straightforward way. It has turned out, that according to the numerical tests mentioned in preceding chapters, the direct approach to solving integral LS equation is in these situations a commensurate equivalent to the partial wave decomposition as can be seen from graphs 3.5–3.8 obtained by Nyström method. Moreover, for higher energies, this computational approach (together with the Chebyshev extension) should be superior to the partial wave decomposition because of the presence of strong forward peaks in the real part of on–shell T–matrix elements hardening its accurate description by means of partial waves (i.e. by Legendre polynomials in the angular variable). Slight complication in these methods is the energy dependent construction of the integration grid having as its main consequence the necessity to perform the whole computation again and again for various energies making the procedure more time consuming.

Another complication buried in the Nyström method consists in the non symmetry of the grid in the q–variable apparent especially for lower energies. In such cases, the grid is very dense in the region $[0, q_0]$, while the converse is true for the interval $[q_0, \infty]$. It is worth to note, that this drawback is dispatched in Chebyshev extension of this method.

Concerning the one–dimensional method (called RLS in this work), we managed to obtain high accuracy close to the machine precision in computation of quantities characterizing the scattering process by using different strategies for local and nonlocal part of the interaction. The local part was treated by means of R–matrix method, while the nonlocal part by the Schwinger–Lanczos iterative al-

gorithm. It was shown that even with relatively low count of mesh points (≈ 100) very accurate results are obtained which can surely compete with the achievements proposed in [20]. Nevertheless, slight numerical modifications of the DVR basis construction were necessary to handle properly potentials unbounded at the origin.

The main drawback of all mentioned methods is the fact, that they can be applied directly only for the relatively simple case of one–channel scattering. The subject of further development would be thus the generalization of these methods in order to be usable also in multi–channel scattering (in this case, the task is typically to solve a set of coupled integral equations), where the lack of algorithms prevails, which wouldn't be based mainly on brute force approach.

Chapter 5

Appendix A

5.1 The NCC rule for a finite interval

In this appendix we would like to briefly introduce an integration scheme based on Gauss type Clenshaw-Curtis quadrature. The full description of this approach is given in the work [12]. The following summary describes the main ideas of this method in the form in which it has been implemented in the present work for the purposes of R-matrix calculations.
What is typically needed in this context is to compute an integral of the following type $\int_{-1}^{1} k(t,s)x(s)\,\mathrm{d}s$, where the kernel $k(t,s)$ is assumed to be so-called *semi-smooth*, i.e.

$$k(t,s) = \begin{cases} k_1(t,s) \text{ for } a \leq s \leq t, \\ k_2(t,s) \text{ for } t \leq s \leq b, \end{cases} \tag{5.1}$$

where $k_{1,2}(t,s) \in C^{p}_{[a,b]\times[a,b]}$ for some $p > 1$.

Without any loss of generality assume that $a = -1$, $b = 1$ and let

$$F(t) = \int_{-1}^{t} k_1(t,s)x(s)\,\mathrm{d}s, \qquad G(t,\lambda) = \int_{-1}^{\lambda} k_1(t,s)x(s)\,\mathrm{d}s \tag{5.2}$$

$$H(t) = \int_{t}^{1} k_1(t,s)x(s)\,\mathrm{d}s, \qquad J(t,\lambda) = \int_{\lambda}^{1} k_1(t,s)x(s)\,\mathrm{d}s. \tag{5.3}$$

Further, assume that for any $t_k \in [a,b]$ the expression $k_1(t_k,s)x(s)$ can be as a function of the variable s expanded in a set of Chebyshev polynomials, i.e., $k_1(t_k,s) = \sum_{i=0}^{n} \alpha_{ki} T_i(s)$. If we consequently write

$$G(t_k,\lambda) = \sum_{j=0}^{n+1} \beta_{kj} T_j(\lambda), \tag{5.4}$$

then according to the work by Clenshaw and Curtis [3], the following relation holds

$$\left[\beta_{k0}, \vdots, \beta_{kn}\right]^T = \mathbf{S}_L \left[\alpha_{k0}, \vdots, \alpha_{kn}\right]^T. \tag{5.5}$$

Similarly, assume that $k_2(t,s)x(s) = \sum_{j=0}^{n} \widetilde{\alpha_{kj}} T_j(s)$. If

$$J(t_k,\lambda) = \int_{\lambda}^{1} k_2(t_k,s)x(s)\,\mathrm{d}s = \sum_{j=0}^{n+1} \widetilde{\beta}_{kj} T_j(\lambda), \tag{5.6}$$

then

$$\left[\widetilde{\beta}_{k0}, \widetilde{\beta}_{k1}, \ldots, \widetilde{\beta}_{kn+1}\right]^T = \mathbf{S}_R \left[\widetilde{\alpha}_{k0}, \widetilde{\alpha}_{k1}, \ldots, \widetilde{\alpha}_{kn}\right]^T, \tag{5.7}$$

where

$$\mathbf{S}_L = \begin{bmatrix} 1 & 1 & -1 & 1 & \cdots & (-1)^n \\ 0 & 1 & 0 & 0 & \cdots & 0 \\ 0 & 0 & 1 & 0 & \cdots & 0 \\ \vdots & \vdots & \vdots & \ddots & \ddots & \vdots \\ 0 & 0 & 0 & 0 & 1 & 0 \\ 0 & 0 & \cdots & 0 & 0 & 1 \end{bmatrix} \begin{bmatrix} 0 & 0 & 0 & 0 & \cdots & 0 \\ 1 & 0 & -\frac{1}{2} & 0 & \cdots & 0 \\ 0 & \frac{1}{4} & 0 & -\frac{1}{4} & \cdots & 0 \\ \vdots & \vdots & \ddots & \ddots & \ddots & \vdots \\ 0 & \cdots & 0 & \frac{1}{2(n-1)} & 0 & -\frac{1}{2(n-1)} \\ 0 & \cdots & 0 & 0 & \frac{1}{2n} & 0 \end{bmatrix},$$

respective

$$\mathbf{S}_R = \begin{bmatrix} 1 & 1 & 1 & 1 & \cdots & 1 \\ 0 & -1 & 0 & 0 & \cdots & 0 \\ 0 & 0 & -1 & 0 & \cdots & 0 \\ \vdots & \vdots & \vdots & \ddots & \ddots & \vdots \\ 0 & 0 & 0 & 0 & -1 & 0 \\ 0 & 0 & \cdots & 0 & 0 & -1 \end{bmatrix} \begin{bmatrix} 0 & 0 & 0 & 0 & \cdots & 0 \\ 1 & 0 & -\frac{1}{2} & 0 & \cdots & 0 \\ 0 & \frac{1}{4} & 0 & -\frac{1}{4} & \cdots & 0 \\ \vdots & \vdots & \ddots & \ddots & \ddots & \vdots \\ 0 & \cdots & 0 & \frac{1}{2(n-1)} & 0 & -\frac{1}{2(n-1)} \\ 0 & \cdots & 0 & 0 & \frac{1}{2n} & 0 \end{bmatrix}$$

is the *left* resp. *right spectral integration matrix.* Let's denote the zeros of T_{n+1} as τ_k and perform a subsitution $\lambda = \tau_k$ for $k = 0, 1, \ldots, n$ in equation (5.4). We obtain after some little tedious algebraic manipulations following formula

$$\begin{bmatrix} G(t_k,\tau_0) \\ \vdots \\ G(t_k,\tau_n) \end{bmatrix} = \mathbf{C}\mathbf{S}_L\mathbf{C}^{-1} \begin{bmatrix} k_1(t_k,\tau_0) & & \\ & \ddots & \\ & & k_1(t_k,\tau_n) \end{bmatrix} \begin{bmatrix} x(\tau_0) \\ \vdots \\ x(\tau_n) \end{bmatrix}. \tag{5.8}$$

And completely analogously its counterpart is obtained, concretely

$$\begin{bmatrix} J(t_k,\tau_0) \\ \vdots \\ J(t_k,\tau_n) \end{bmatrix} = \mathbf{C}\mathbf{S}_R\mathbf{C}^{-1} \begin{bmatrix} k_2(t_k,\tau_0) & & \\ & \ddots & \\ & & k_2(t_k,\tau_n) \end{bmatrix} \begin{bmatrix} x(\tau_0) \\ \vdots \\ x(\tau_n) \end{bmatrix}, \tag{5.9}$$

where the symbol $\mathbf{C}$ stands for the so-called *discrete cosine transformation matrix*, i.e.

$$\mathbf{C}_{kj} = T_j(\tau_k), \qquad j,k = 0, 1, \ldots, n.$$

This matrix has orthogonal columns $\mathbf{C}^T\mathbf{C} = \mathrm{diag}(n, n/2, \ldots, n/2)$. Therefore $\mathbf{C}^{-1} = \mathrm{diag}(1, 2, \ldots, 2)/n\mathbf{C}^T$.
Since by definition $F(\tau_k) = G(\tau_k, \tau_k)$, we get

$$F(\tau_k) = [0, \ldots, 0, 1, 0, \ldots, 0]\,\mathbf{C}\mathbf{S}_L\mathbf{C}^{-1} \begin{bmatrix} k_1(t_k, \tau_0) & & \\ & \ddots & \\ & & k_1(t_k, \tau_n) \end{bmatrix} \begin{bmatrix} x(\tau_0) \\ \vdots \\ x(\tau_n) \end{bmatrix}$$
$$= [w_{k0}, w_{k1}, \ldots, w_{kn}] \begin{bmatrix} k_1(t_k, \tau_0) & & \\ & \ddots & \\ & & k_1(t_k, \tau_n) \end{bmatrix} \begin{bmatrix} x(\tau_0) \\ \vdots \\ x(\tau_n) \end{bmatrix},$$

where $[w_{k0}, \ldots, w_{kn}]$ stands for the $(k+1)$−st row of the matrix $\mathbf{W} \stackrel{\mathrm{def}}{=} \mathbf{C}\mathbf{S}_L\mathbf{C}^{-1}$. By the means of the Schur matrix product $(\mathbf{A} \circ \mathbf{B})_{ij} = \mathbf{A}_{ij}\mathbf{B}_{ij}$, the previous formula can be restated as

$$\begin{bmatrix} F(\tau_0) \\ \vdots \\ F(\tau_n) \end{bmatrix} = (\mathbf{W} \circ \mathbf{K}_1) \begin{bmatrix} x(\tau_0) \\ \vdots \\ x(\tau_n) \end{bmatrix}, \tag{5.10}$$

where $\mathbf{K}_1 = (k_1(\tau_i, \tau_j))_{i,j=0}^n$. Analogously

$$\begin{bmatrix} H(\tau_0) \\ \vdots \\ H(\tau_n) \end{bmatrix} = (\mathbf{V} \circ \mathbf{K}_2) \begin{bmatrix} x(\tau_0) \\ \vdots \\ x(\tau_n) \end{bmatrix}, \tag{5.11}$$

where $\mathbf{V} \stackrel{\mathrm{def}}{=} \mathbf{C}\mathbf{S}_R\mathbf{C}^{-1}$. To generalize this scheme for an other interval $[a, b]$ other than $[-1, 1]$ we employ linear transfomation $h(\tau) = (b-a)/2\tau + (a+b)/2$. If we consequently denote $\eta_j = h(\tau_j)$ and

$$F_a(t) = \int_a^t k_1(t, s)x(s)\,\mathrm{d}s, \qquad H_b(t) = \int_t^b k_1(t, s)x(s)\,\mathrm{d}s, \tag{5.12}$$

we become

$$\begin{bmatrix} F_a(\tau_0) \\ \vdots \\ F_a(\tau_n) \end{bmatrix} = \frac{b-a}{2} (\mathbf{W} \circ \mathbf{K}_1) \begin{bmatrix} x(\tau_0) \\ \vdots \\ x(\tau_n) \end{bmatrix}, \tag{5.13}$$

and

$$\begin{bmatrix} H_b(\tau_0) \\ \vdots \\ H_b(\tau_n) \end{bmatrix} = \frac{b-a}{2} (\mathbf{V} \circ \mathbf{K}_2) \begin{bmatrix} x(\tau_0) \\ \vdots \\ x(\tau_n) \end{bmatrix}. \tag{5.14}$$

5.2 The NCC composite rule for a finite interval

However, if the integration range would be too large, spectral matrices of high order would be required to calculate the integral properly. To compensate for this natural drawback, we have used a composite rule introduced below. Again, the quest is to be able to evaluate the integral $y(t) \equiv \int_a^b k(t,s)x(s)\,\mathrm{d}s$ with a semi-smooth kernel as a function of t. To this end decompose the original interval $[a,b]$ into m sectors

$$a \equiv b_0 < b_1 < b_2 < \cdots < b_m \equiv b,$$

and define

$$x(t) = \begin{cases} x_1(t) \text{ if } t \in [b_0, b_1] \\ x_2(t) \text{ if } t \in (b_1, b_2] \\ \vdots \\ x_1(t) \text{ if } t \in (b_{m-1}, b_m] \end{cases}$$

and

$$y(t) = \begin{cases} y_1(t) \text{ if } t \in [b_0, b_1] \\ y_2(t) \text{ if } t \in (b_1, b_2] \\ \vdots \\ y_m(t) \text{ if } t \in (b_{m-1}, b_m] \end{cases}.$$

In this notation we can rewrite the defining equation for $y(t)$ as

$$\begin{aligned} y_j(t) = &\int_{b_0}^{b_1} k_1(t,s)x_1(s)\,\mathrm{d}s + \ldots + \int_{b_{j-1}}^{t} k_1(t,s)x_j(s)\,\mathrm{d}s + \\ &+ \int_{t}^{b_j} k_2(t,s)x_j(s)\,\mathrm{d}s + \ldots + \int_{b_{m-1}}^{b_m} k_2(t,s)x_m(s)\,\mathrm{d}s. \end{aligned} \tag{5.15}$$

By using the machinery of the previous subsection to each of the integrals we find, that the previous equation is equivalent to

$$\begin{aligned} \overline{y}_j = &\frac{b_1 - b_0}{2}\left[(\mathbf{W}+\mathbf{V}) \circ \mathbf{K}_{1j}\right]\overline{x}_1 + \ldots + \frac{b_j - b_{j-1}}{2}\left[\mathbf{W} \circ \mathbf{K}_{jj} + \mathbf{V} \circ \tilde{\mathbf{K}}_{jj}\right]\overline{x}_j \\ &+ \ldots + \frac{b_m - b_{m-1}}{2}\left[(\mathbf{W}+\mathbf{V}) \circ \mathbf{K}_{mj}\right]\overline{x}_m, \end{aligned} \tag{5.16}$$

where

$$\overline{x}_j = \left[x(\tau_0^{(j)}), x(\tau_1^{(j)}), \cdots, x(\tau_{n_j}^{(j)})\right]^T, \qquad \overline{y}_j = \left[y(\tau_0^{(j)}), y(\tau_1^{(j)}), \cdots, y(\tau_{n_j}^{(j)})\right]^T$$

and

$$\mathbf{K}_{jj} = \left(k_1\left(\tau_p^{(j)}, \tau_q^{(j)}\right)\right)_{p,q=0}^{n_j} \qquad \tilde{\mathbf{K}}_{jj} = \left(k_2\left(\tau_p^{(j)}, \tau_q^{(j)}\right)\right)_{p,q=0}^{n_j},$$
$$\mathbf{K}_{ij} = \left(k_1\left(\tau_p^{(j)}, \tau_q^{(i)}\right)\right)_{p,q=0}^{n_j,n_i} \text{ if } i < j,$$
$$\mathbf{K}_{ij} = \left(k_2\left(\tau_p^{(j)}, \tau_q^{(i)}\right)\right)_{p,q=0}^{n_j,n_i} \text{ if } i > j.$$

This approach has been used in the implementation of the R-matrix method. The whole integration interval $[0, R_{max}]$ has been divided into several sectors as described above. However, these sectors don't need to coincide with the sectors in the R-matrix sense. On the contrary, it turns out, that an accuracy improvement is achieved in the case when a few (say 2–4) sectors in the sense of this quadrature scheme are virtually merged into one R-matrix sector.

Chapter 6

Appendix B

In the framework of the Nyström method, we need to calculate the phase shifts for a given angular momentum. The method used for this task is based on direct integration of the radial Schrödinger equation and consequent examination of the asymptotics of the constructed solution. Common method used to integrate second order differential equations $y'' = f(r,y)y(r)$, where f doesn't depend on the first derivate of y, is the famous fifth order two step Numerov method

$$y_{n+1} - 2y_n + y_{n-1} = \frac{1}{12}h^2 \left[f(r_{n+1})y_{n+1} + 10f(r_n)y_n + f(r_{n-1})y_{n-1} \right], \qquad (6.1)$$

where the common abbreviation $y_n \equiv r_n, r_n = nh$ has been used.

The superiority of this method over the family of Runge-Kutta methods lies in the fact, that the right hand side of the original differential equation needs to be numerically evaluated only once at each step. Assuming further that the function $f(r,y)$ is linear in $y(r)$ we can restate the original differential equation as $y'' = U(r) + V(r)y$, where $U(r)$ and $V(r)$ are some arbitrary continuous functions of the radial variable r. Substituting this assumption in the equation (6.1) yields after some manipulations following explicit scheme for the value of the solution y at the point r_{n+1}, which is expressed by the virtue of the $y-$values at the two preceding grid points. Namely

$$y_{n+1} = \frac{2y_n - y_{n-1} + \frac{h^2}{12}\left(U_{n+1} + 10F_n + F_{n-1}\right)}{1 - \frac{h^2}{12}V_{n+1}} \qquad (6.2)$$

Natural question arising at this point is how to start the method, i.e. how to specify the boundary conditions at the origin. When we are examining only the asymptotics of the solution then the normalization of the entire solution is clearly irrelevant. Because of this reason we set $y_0 = 0$ (y has the meaning of the radial part of the wave function) and $y_1 = 1$ (this value can be choosen completely arbitrary) in our calculations.

More difficult is the case, when we need to specify the value together with the first derivative of the solution at the origin. Because the global error of the

Numerov method is of order $\mathcal{O}(h^5)$, we need to express the value y_1 at least with this accuracy. The following algorithm represents an elegant way how to cope with this issue (in the expressions below, the symbol f_n stands for $f(r_n, y(r_n))$). We will seek y_1 in the form

$$y_1 = y_0 + hy_0{}' + h^2(af_0 + bf_1 + cf_2), \tag{6.3}$$

where a, b, c are yet undetermined coefficients. The quantities $f_{1,2}$ can be further expressed by the means of Taylor expansion as

$$\begin{aligned} f_1 &= f_0 + hf_0{}' + \frac{h^2}{2} f_0{}'' + \mathcal{O}(h^3), \\ f_2 &= f_0 + 2hf_0{}' + 2h^2 f_0{}'' + \mathcal{O}(h^3). \end{aligned} \tag{6.4}$$

Substituting these relations into equation (6.3) yields after some algebraic manipulations

$$y_1 = y_0 + hy_0{}' + h^2(a+b+c)f_0 + h^3(b+2c)f_0{}' + h^4(\frac{b}{2} + 2c)f_0{}'' + \mathcal{O}(h^5). \tag{6.5}$$

When we compare this expansion in powers of h with the standard Taylor expansion and solve the obtained equations for a, b, c, we find out, that $a = 7/24, b = 1/4, c = -1/24$. Thus we have

$$y_1 = y_0 + hy_0{}' + \frac{h^2}{24}(7f_0 + 6f_1 - f_2). \tag{6.6}$$

According to the main Numerov algorithm y_2 should be give as

$$y_2 = \frac{2y_1 - y_0 + \frac{h^2}{12}(U_2 + 10F_1 + F_0)}{1 - \frac{h^2}{12}V_2}. \tag{6.7}$$

We see, that (6.6) together with (6.7) constitute a system of two linear equations for the unknown values y_1 and y_2. Some algebra gives the sought quantity y_1 indeed with the desired accuracy. Namely,

$$y_1 = \frac{y_0\left(1 - \frac{h^2}{24}V_2\right) + hy_0{}'\left(1 - \frac{h^2}{12}V_2\right) + \frac{h^2}{24}(7f_0 + 6U_1 - U_2) - \frac{h^4}{36}V_2(f_0 + 2U_1)}{1 - \frac{h^2}{4}V_1 + \frac{h^4}{18}V_1V_2}. \tag{6.8}$$

The more complex sixth order alternative (Cash, Raptis - [19]) to the Numerov method can be written as

$$\begin{aligned} y_{n+1} - 2y_n + y_{n-1} = \frac{1}{60}h^2\Big\{ & f(r_{n+1})y_{n+1} + f(r_{n-1})y_{n-1} + 26f(r_n)y_n + \\ & 16\left[f(r_{n+1/2})y_{n+1/2} + f(r_{n-1/2})y_{n-1/2}\right]\Big\}, \end{aligned}$$

where

$$y_{n+1/2} = \frac{1}{104}\{5y_{n+1} + 146y_n - 47y_{n-1}\} + \frac{1}{4992}h^2\left[-59f(r_{n+1})y_{n+1} + 1438f(r_n)y_n + 253f(r_{n-1})y_{n-1}\right]$$

and

$$y_{n-1/2} = \frac{1}{52}\{3y_{n+1} + 20y_n + 29y_{n-1}\} + \frac{1}{4992}h^2\left[41f(r_{n+1})y_{n+1} - 682f(r_n)y_n - 271f(r_{n-1})y_{n-1}\right].$$

An alternative approach to the numerical problem of phase shifts computations is summarized in the work [6]. The method presented in this paper completely avoids the necessity of solving the second order differential equation by converting it to the corresponding integral form and examining the asymptotics of its solution. The main drawback of this method is however the necessary knowledge of the second Born off-shell matrix elements making this method less convenient for cumbersome potentials, for which these elements need to be computed numerically.

Bibliography

[1] Abramowitz M., Stegun I. A.: *Handbook of Mathematical Functions*, Dover Publications Inc., New York, 1972

[2] Adhikari S. K., Kowalski K. L.: *Dynamical Collision theory and its Applications*, Academic Press Inc., San Diego, 1991.

[3] Clenshaw C. W., Curtis A. R.: *A method for numerical integration on an automatic computer*, Num. Math. **2** (1960) 197–205.

[4] Elster Ch., Thomas J. H., Glöckle W.: *Two-Body T-Matrices without Angular-Momentum Decomposition: Energy and Memonetum Dependences*, Few-Body Systems **24** (1998) 55–79.

[5] Gonzales R. A., Eisert J., Koltracht I., Rawithser G.: *Integral equation method for the Continuous Spectrum Radial Schrödinger equation*, J. Comput. Phys. **134** (1997) 134–139.

[6] Holt A.R., Santoso B.: *A Fredholm integral equation method for scattering phase shifts*, J. Phys. B. **5** (1972) 497–507.

[7] Horáček J., Bok J.: *K-matrix calculation for general nonlocal potentials*, Comput. Phys. Commun. **59** (1990) 319–323.

[8] Horáček J., Sasakawa T.: *Method of continued fractions with application to atomic physics*, Phys. Rev. A **28** (1983) 2151–2156.

[9] Horáček J., Sasakawa T.: *Method of continued fractions with application to atomic physics II*, Phys. Rev. A **30** (1984) 2274–2277.

[10] Horáček J., Sasakawa T.: *Method of continued fractions for on- and off-shell t matrix of local and nonlocal potentials*, Phys. Rev. C **32** (1985) 70–75.

[11] Holler E. W., Allen L. J.: *Method of continued fractions for complex potentials*, Phys. Rev. A **33** (1986) 4393–4394.

[12] Kang S.-Y., Koltracht I., Rawitscher G.: *Nyström-Clenshaw-Curtis quadrature for integral equations with discontinuous kernels*, Math. Comp. **72** (2002) 729–756.

[13] Kim T., Udagawa T.: *Method for nonlocal optical model calculations*, Phys. Rev. C **42** (1990) 1147–1149.

[14] Lippmann B. A., Schwinger J.: *Variational Principles for Scattering Processes. I*, Phys. Rev. **79** (1950) 469–480.

[15] Meyer H.-D., Horáček J., Cederbaum L. S.: *Schwinger and anomaly-free Kohn variational principles and a generalized Lanczos algorithm for non symmetric operators*, Phys. Rev. A **43** (1991) 3587–3596.

[16] Mil'nikov G. V., Nakamura H. Horáček J.: *Stable and efficient evaluation of Green's function in scattering problem*, Comput. Phys. Commun. **135** (2001) 278–292.

[17] Newton R. G.: *Scattering theory of waves and particles*, McGraw-Hill Inc., New York, 1966.

[18] Raptis A. D., Cash J. R.: *A high order method for the numerical integration of the one dimensional Schrödinger equation*, Comput. Phys. Commun. **33** (1984) 299–304.

[19] Raptis A. D., Cash J. R.: *A variable step method for the numerical integration of the one dimensional Schrödinger equation*, Comput. Phys. Commun. **36** (1985) 113–119.

[20] Rawitscher G. H., Kang S.-Y., Koltracht I.: *A novel method for the solution of the Schrödinger equation in the presence of exchange terms*, J. Chem. Phys. **118** (2003) 9149–9156.

[21] Sams W. N., Kouri D. J.: *Noniterative Solutions of Integral Equations for Scattering. I. Single Channels*, J. Chem. Phys. **51** (1969) 4809–4813.